Search for heavy long-lived charged particles in pp collisions at $\sqrt{s} = 7TeV$

CMS Collaboration ; Chatrchyan, S ; Khachatryan, V ; Aguiló, E ; Amsler, C ; Chiochia, V ; De Visscher, S ; Favaro, C ; Ivova Rikova, M ; Millan Mejias, B ; Otiougova, P ; Robmann, P ; Snoek, H ; Tupputi, S ; Verzetti, M ; et al

Abstract: The result of a search for heavy long-lived charged particles produced in pp collisions at View the MathML source at the LHC is described. The data sample has been collected using the CMS detector and corresponds to an integrated luminosity of 5.0 fb−1. The inner tracking detectors are used to define a sample of events containing tracks with high momentum and high ionization energy loss. A second sample of events, which have high-momentum tracks satisfying muon identification requirements in addition to meeting high-ionization and long time-of-flight requirements, is analyzed independently. In both cases, the results are consistent with the expected background estimated from data. The results are used to establish cross section limits as a function of mass within the context of models with long-lived gluinos, scalar top quarks and scalar taus. Cross section limits on hyper-meson particles, containing new elementary long-lived hyper-quarks predicted by a vector-like confinement model, are also presented. Lower limits at 95% confidence level on the mass of gluinos (scalar top quarks) are found to be 1098 (737) GeV/c2. A limit of 928 (626) GeV/c2 is set for a gluino (scalar top quark) that hadronizes into a neutral bound state before reaching the muon detectors. The lower mass limit for a pair produced scalar tau is found to be 223 GeV/c2. Mass limits for a hyper-kaon are placed at 484, 602, and 747 GeV/c2 for hyper- masses of 800, 1200, and 1600 GeV/c2, respectively.

DOI: https://doi.org/10.1016/j.physletb.2012.06.023,

EUROPEAN ORGANIZATION FOR NUCLEAR RESEARCH (CERN)

CERN-PH-EP/2012-093
2013/01/25

CMS-EXO-11-022

Search for heavy long-lived charged particles in pp collisions at $\sqrt{s} = 7\,\text{TeV}$

The CMS Collaboration*

Abstract

The result of a search for heavy long-lived charged particles produced in pp collisions at $\sqrt{s} = 7\,\text{TeV}$ at the LHC is described. The data sample has been collected using the CMS detector and corresponds to an integrated luminosity of $5.0\,\text{fb}^{-1}$. The inner tracking detectors are used to define a sample of events containing tracks with high momentum and high ionization energy loss. A second sample of events, which have high-momentum tracks satisfying muon identification requirements in addition to meeting high-ionization and long time-of-flight requirements, is analyzed independently. In both cases, the results are consistent with the expected background estimated from data. The results are used to establish cross section limits as a function of mass within the context of models with long-lived gluinos, scalar top quarks and scalar taus. Cross section limits on hyper-meson particles, containing new elementary long-lived hyper-quarks predicted by a vector-like confinement model, are also presented. Lower limits at 95% confidence level on the mass of gluinos (scalar top quarks) are found to be 1098 (737) GeV/c^2. A limit of 928 (626) GeV/c^2 is set for a gluino (scalar top quark) that hadronizes into a neutral bound state before reaching the muon detectors. The lower mass limit for a pair produced scalar tau is found to be $223\,\text{GeV}/c^2$. Mass limits for a hyper-kaon are placed at 484, 602, and $747\,\text{GeV}/c^2$ for hyper-ρ masses of 800, 1200, and $1600\,\text{GeV}/c^2$, respectively.

Submitted to Physics Letters B

*See Appendix A for the list of collaboration members

1 Introduction

Various extensions to the standard model (SM) of particle physics allow for the possibility that as-yet-undiscovered massive ($\gtrsim$100 GeV/c^2) elementary particles could be long-lived with lifetime greater than $\sim$1 ns as a result of a new conserved quantum number, a kinematic constraint or a weak coupling [1–3]. Such particles, where they are electrically charged, are referred to as Heavy Stable Charged Particles (HSCP) in this article. Because of their high mass, a significant fraction of the HSCPs that could be produced at the Large Hadron Collider (LHC) are expected to be detectable as high momentum (p) tracks with an anomalously large rate of energy loss through ionization ($\mathrm{d}E/\mathrm{d}x$) and an anomalously long time-of-flight (TOF).

Previous collider searches for HSCPs have been performed at LEP [4–7], HERA [8], the Tevatron [9–15], and the LHC [16–21]. HSCPs are expected to reach the outer muon systems of the collider detectors even if they are strongly interacting. In that case it is expected that a bound state (R-hadron) is formed in the process of hadronization [22–24] and that the energy loss occurs primarily through low momentum transfer interactions [1, 25–27], allowing the R-hadron to traverse an amount of material typical of the calorimeter of a collider experiment. However, the nuclear interactions experienced in matter by an R-hadron may lead to charge exchange. A recent study [28] of the modeling of nuclear interactions of HSCPs favours a scenario in which the majority of the R-hadrons containing a gluino, $\widetilde{\mathrm{g}}$ (the supersymmetric partner of the gluon), or a bottom squark would emerge neutral in the muon detectors. Given the large uncertainties in the nuclear interactions experienced by R-hadrons, experimental strategies that do not rely on a muon-like behavior of HSCPs are important. Two strategies already employed are to search for very slow ($\beta \lesssim 0.4$) R-hadrons brought to rest in the detector [12, 16, 21], and to search using only inner tracker and/or calorimeter information [17–19].

In this article we present a search for HSCPs produced in pp collisions at $\sqrt{s} = 7$ TeV at the LHC, recorded using the Compact Muon Solenoid (CMS) detector [29]. The search is based on a data sample collected in 2011, corresponding to an integrated luminosity of 5.0 fb^{-1}. Events were collected using either of two triggers, one based on muon transverse momentum (p_{T}) and the other based on the missing transverse energy ($E_{\mathrm{T}}^{\mathrm{miss}}$) in the event. This event sample was then used for two separate selections. In the first, the HSCP candidates were defined as tracks reconstructed in the inner tracker detector with large $\mathrm{d}E/\mathrm{d}x$ and high p_{T}. In the second, the tracks were also requested to be associated with identified muons that had a long time-of-flight as measured by the muon detectors. The first selection is largely insensitive to the uncertainties in modeling the R-hadron nuclear interactions. For both selections, the mass of the candidate was calculated from the measured values of p and $\mathrm{d}E/\mathrm{d}x$. This analysis extends our previously published result [17] through the use of a larger dataset, muon TOF information, and track isolation requirements. This new analysis also probes additional signal models.

2 Signal benchmarks

The results of this search have been interpreted within the context of several theoretical models. Supersymmetric models [30, 31] can in some cases allow for HSCP candidates in the form of gluinos, scalar top quarks (stops, $\widetilde{\mathrm{t}}_1$, the supersymmetric partner of the top quark), and scalar taus (stau, $\widetilde{\tau}_1$, the supersymmetric partner of the τ). We also consider a new model that postulates a QCD-like confinement force between new elementary particles (hyper-quarks, $\widetilde{q}$) [32] and allows for long-lived hyper-mesons.

In order to study the uncertainties related to the underlying production processes, samples were produced with three different multiparton interaction (MPI) models [33]: DW with CTEQ5L

parton distribution functions (PDF) [34] (used in [19]), D6T with CTEQ6L1 PDF [35] (used in [17]), and Z2 with CTEQ6L1 PDF. The latter model features a harder initial-state radiation spectrum. The final results of this analysis are obtained with samples using the D6T MPI, which yield the most conservative signal selection efficiency of the three choices.

Gluino and stop production were modelled as pair production over the particle mass range 130–1200 GeV/c^2 using PYTHIA v6.422 [36]. For $\widetilde{\mathrm{g}}$ production, we set the squark masses to very high values (>7 TeV) to reflect the scenario of split supersymmetry [37, 38]. The fraction f of produced $\widetilde{\mathrm{g}}$ hadronizing into a $\widetilde{\mathrm{g}}$-gluon state (R-gluonball) is an unknown parameter of the hadronization model and affects the fraction of R-hadrons that are produced as neutral particles. As in [17], results were obtained for two different values of f, 0.1 and 0.5. Unless specified otherwise, the value $f = 0.1$ is assumed. The interactions of the HSCPs using the CMS apparatus and the detector response were simulated in detail with the GEANT4 v9.2 [39, 40] toolkit. Two scenarios for R-hadron strong interactions with matter were considered: the first follows the model defined in [27, 41], while the second is one of complete charge suppression, where any nuclear interaction of the R-hadron causes it to become neutral. In the second scenario, effectively all R-hadrons are neutral by the time they enter the muon system.

The minimal gauge-mediated supersymmetry breaking (GMSB) model [42] was used to describe $\widetilde{\tau}_1$ production, which can proceed either via direct pair production or via production of heavier supersymmetric particles that decay to one or more $\widetilde{\tau}_1$. The latter process has a larger cross section than direct production. Two benchmark points on the Snowmass Points and Slopes line 7 [43] have been considered. They correspond to $N = 3$ chiral SU(5) multiplets added to the theory at the scales $F = 100$ and 160 TeV [42] respectively, and an effective supersymmetry-breaking scale $\Lambda = 50$ and 80 TeV respectively. Both points have the ratio of neutral Higgs field vacuum expectation values $\tan\beta = 10$, a positive sign for the Higgs-Higgsino mass parameter ($\mathrm{sgn}(\mu) = 1$), and the ratio of the gravitino mass to the value it would have if the only supersymmetry breaking scale were that in the messenger sector, $c_{\mathrm{grav}} = 10^4$. The particle mass spectrum and the decay table were produced with the program ISASUGRA version 7.69 [44]. The resulting $\widetilde{\tau}_1$ masses are 156 and 247 GeV/c^2, and the squark and gluino masses are about 1.1 and 1.7 TeV/c^2, respectively. Additional mass points in the range 100 to 500 GeV/c^2 were obtained by varying the Λ parameter in the range 31 to 100 TeV and keeping the ratio of F to Λ equal to 2. In addition, direct $\widetilde{\tau}_1$ pair production samples were generated separately.

As mentioned above, another HSCP benchmark considered in this paper is a vector-like confinement model that postulates a QCD-like confinement force between new elementary particles (hyper-quarks, $\widetilde{q}$) [32]. The hyper-quarks can be confined into SM hadron-like hyper-mesons such as hyper-π ($\widetilde{\pi}$), hyper-K ($\widetilde{\mathrm{K}}$), or hyper-ρ ($\widetilde{\rho}$). We assume a simplified model (similar to that in Section 4.2 of Ref. [32]) with $\widetilde{\pi}$ or $\widetilde{\mathrm{K}}$ pair production via either the Drell–Yan process ($\widetilde{\mathrm{K}}\,\overline{\widetilde{\mathrm{K}}}$) or via production of a resonant $\widetilde{\rho}$ ($\widetilde{\rho} \to \widetilde{\mathrm{K}}\,\overline{\widetilde{\mathrm{K}}}$) analogous to QCD ρ meson production [45]. The $\widetilde{\rho}$ mixes only with the electroweak gauge bosons, and therefore is not produced strongly. In this model, the $\widetilde{\pi}$ is short-lived and decays to SM gauge bosons (e.g. $\widetilde{\pi} \to W^{\pm}\gamma$, $\widetilde{\pi} \to W^{\pm}Z$). Its production processes are not included in the simulation. However, the $\widetilde{\mathrm{K}}$ is long-lived compared to the detector size and constitutes an HSCP candidate. In the considered model, the $\widetilde{\mathrm{K}}$, like the $\widetilde{\tau}_1$, would only interact via the electroweak force. The mix of resonant and Drell-Yan production results in different kinematics, compared to the GMSB $\widetilde{\tau}_1$ model. For $\widetilde{\mathrm{K}}$ mass values much less than half the $\widetilde{\rho}$ mass, the HSCP receives a significant boost from the resonance decay [46], while near threshold the $\widetilde{\mathrm{K}}$ is slow enough that the acceptance drops dramatically. Parton-level events were generated with CALCHEP v2.5.4 [47] and passed to PYTHIA

for hadronization and simulation of the underlying event. The masses of the $\widetilde{\mathrm{K}}$, $\widetilde{\pi}$, and $\widetilde{\rho}$ are treated as free parameters in the model, affecting in particular the $\widetilde{\rho}$ width. We used a fixed $\widetilde{\pi}$ mass of 600 GeV/c^2 and $\widetilde{\mathrm{K}}$ masses in the range 100 to 900 GeV/c^2, for $\widetilde{\rho}$ masses of 800, 1200 and 1600 GeV/c^2.

In all simulated samples, the primary collision event was overlaid with simulated minimum-bias events to reproduce the distribution of the number of inelastic collisions per bunch crossing (pile-up) observed in data.

3 The CMS detector

A detailed description of the CMS detector can be found elsewhere [29]. The central feature of the CMS apparatus is a superconducting solenoid of 6 m internal diameter. Within the field volume are the silicon pixel and strip inner tracking detectors, the crystal electromagnetic calorimeter (ECAL), and the brass/scintillator hadron calorimeter (HCAL). Muons are measured in gas-ionization detectors embedded in the steel return yoke. In addition to the barrel and endcap detectors, CMS has extensive forward calorimetry. CMS uses a right-handed coordinate system, with the origin at the nominal interaction point, the x axis pointing to the center of the LHC ring, the y axis pointing up (perpendicular to the LHC plane), and the z axis along the counterclockwise-beam direction. The polar angle, θ, is measured from the positive z axis and the azimuthal angle, ϕ, is measured in the x-y plane. The muons are measured in the pseudorapidity ($\eta \equiv -\ln\tan(\theta/2)$) range $|\eta| < 2.4$, with detection planes made using three technologies: drift tubes (DT), cathode strip chambers (CSC), and resistive plate chambers (RPC). The DT and CSC detectors are installed in the barrel at $|\eta| < 1.2$ and in the endcaps at $0.9 < |\eta| < 2.4$, respectively, whereas RPCs cover the range $|\eta| < 1.6$. The inner tracker measures charged particle trajectories within the pseudorapidity range $|\eta| < 2.5$. It consists of 1440 silicon pixel modules and 15 148 silicon strip modules. The p_{T} resolution for tracks measured in the central (forward) region of the silicon tracker is 1% (2%) for p_{T} values up to 50 GeV/c and degrades to 10% (20%) at p_{T} values of 1 TeV/c. The CMS trigger consists of a two-stage system. The first level (L1) of the CMS trigger system, composed of custom hardware processors, uses information from the calorimeters and muon detectors to select a subset of the events. The High Level Trigger (HLT) processor farm further decreases the event rate from around 100 kHz to around 300 Hz, before data storage.

3.1 $\mathrm{d}E/\mathrm{d}x$ Measurement

The $\mathrm{d}E/\mathrm{d}x$ measurement for a candidate track was performed using the charge information contained in the track measurements provided by the silicon strip and pixel detectors. A silicon strip or pixel measurement consists of a cluster of adjacent strips or pixels with a charge above threshold. These clusters form the basis for $\mathrm{d}E/\mathrm{d}x$ measurements in this analysis. For $\mathrm{d}E/\mathrm{d}x$ measurement purposes, a 'cleaning procedure' was applied to the clusters found in the silicon strip detectors. This selection is intended to reduce anomalous ionization contributions due to overlapping tracks, nuclear interactions, and hard δ-rays in the silicon strip detectors. Genuine single particles release charge primarily within one or two neighbouring strips. Other strips generally carry only a fraction (to a first approximation equal to 10^{-n}, where n is the distance in units of strips) of the total cluster charge from capacitive coupling and cross-talk effects [48]. Measurements displaying multiple charge maxima or more than two adjacent strips containing comparable charge were therefore not used in the $\mathrm{d}E/\mathrm{d}x$ calculations. This cleaning procedure, which discards on average about 20% of the track measurements, rejects background at high $\mathrm{d}E/\mathrm{d}x$ without a significant impact on the signal acceptance.

As in [17], a modified version of the Smirnov–Cramer–von Mises [49, 50] discriminant was used for estimating the degree of compatibility of the observed charge measurements with those expected for particles close to the minimum of ionization:

$$I_{\text{as}} = \frac{3}{J} \times \left\{ \frac{1}{12J} + \sum_{i=1}^{J} \left[P_i \times \left(P_i - \frac{2i-1}{2J} \right)^2 \right] \right\}, \tag{1}$$

where J is the number of track measurements in the silicon-strip detectors, P_i is the probability for a particle close to the minimum of ionization to produce a charge smaller or equal to that of the i–th measurement for the observed path length in the detector, and the sum is over the track measurements ordered in terms of increasing P_i. The charge probability density functions used to calculate P_i were obtained using reconstructed tracks with $p_{\text{T}} > 5\,\text{GeV}/c$ in events collected with a minimum bias trigger. As in [17], the most probable value of the particle $\text{d}E/\text{d}x$ was determined using a harmonic estimator I_{h}:

$$I_{\text{h}} = \left(\frac{1}{N} \sum_{i=1}^{N} (c_i)^{-2} \right)^{-1/2}, \tag{2}$$

where N is the total number of track measurements in the pixel and silicon-strip detectors and c_i is the charge per unit path length of the i-th measurement. As implied above, the I_{h} estimator was computed using both silicon strip and pixel measurements, whereas the I_{as} estimator was based only on silicon strip measurements. As in [17], the mass measurement was based on the formula:

$$I_{\text{h}} = K \frac{m^2}{p^2} + C, \tag{3}$$

where the empirical parameters $K = 2.559 \pm 0.001\,\text{MeV}\,\text{cm}^{-1}\,c^2$ and $C = 2.772 \pm 0.001\,\text{MeV}\,\text{cm}^{-1}$ were determined from data using a sample of low-momentum protons [51]. Equation (3) reproduces the Bethe-Bloch formula [52] with an accuracy of better than 1% in the range $0.4 < \beta < 0.9$, which corresponds to $1.1 < (\text{d}E/\text{d}x)/(\text{d}E/\text{d}x)_{\text{MIP}} < 4.0$, where $(\text{d}E/\text{d}x)_{\text{MIP}}$ is the ionization energy loss rate of a particle at the minimum of ionization. Equation (3) implicitly assumes that the HSCP candidates have unit charge. For HSCPs with masses above $100\,\text{GeV}/c^2$, the mass resolution is expected to degrade gradually with increasing mass. This effect is due to the deterioration of the momentum resolution and to the limit on the maximum charge that can be measured by the silicon strip tracker analogue-to-digital converter modules, which also affects the mass scale. These effects are modeled in the simulation. For an HSCP with a mass of $300\,\text{GeV}/c^2$, the mass resolution and the most probable reconstructed mass were found to be 16% and $280\,\text{GeV}/c^2$, respectively.

For each reconstructed track with momentum p as measured in the inner tracker, I_{as}, I_{h} and m were computed using Eq. (1), (2), and (3). These values were used in the candidate selection as described in Sections 4 and 5.

3.2 TOF Measurement

A major addition to this analysis with respect to that in Ref. [17] is the use of TOF information from the muon system. The β measurement for a candidate track was performed using time information provided by the individual DT and CSC track measurements. The DT system consists of four layers of muon chambers interleaved with the return yoke of the solenoid. The chambers in the three innermost layers contain three super-layers (SL) each, two of them measuring the track ϕ projection and the third measuring the θ projection. The chamber in the

outermost layer is equipped with just two SLs that measure the track ϕ projection. Each SL is composed of four DT layers. For TOF measurement purposes, only SLs providing measurements in the ϕ projection were used because their time resolution is a factor of two better than that of the θ-projection SLs. The CSC system comprises four layers of chambers at increasing $|z|$ positions. Each chamber contains six detection layers. All detection layers were used for TOF measurement purposes.

Both the DTs and CSCs measure the difference (δ_t) between the particle crossing time and the average time at which a high-momentum muon, produced at the nominal collision point in the triggered bunch crossing, would pass through the same portion of the detector. Measurements from prompt HSCPs would yield a δ_t greater than zero. The ϕ-projection DT measurements within a chamber were fitted with a straight line. In order to improve the accuracy of the parameters of the straight line for late tracks, a time shift common to all measurements within the chamber was introduced as a third free parameter of the fit. Having four chambers with eight layers measuring the track ϕ projections, there are up to 32 independent DT δ_t measurements along a candidate track. Each detection layer in a CSC chamber has a nearly orthogonal layout of anode wires and cathode strips. The arrival time of the signals from both the anode wires and cathode strips measures the particle δ_t. Having four chambers, six detection layers per chamber, and two δ_t measurements per layer, there are up to 48 independent CSC δ_t measurements along a candidate track.

A single δ_t measurement can be used to determine the track β^{-1} via the equation:

$$\beta^{-1} = 1 + \frac{c\delta_t}{L} \tag{4}$$

where L is the flight distance and c is the speed of light. The track β^{-1} value was calculated as the weighted average of the β^{-1} measurements associated with the track. The weight for the i^{th} DT measurement is given by:

$$w_i = \frac{(n-2)}{n}\frac{L_i^2}{\sigma_{DT}^2} \tag{5}$$

where n is the number of ϕ projection measurements found in the chamber from which the measurement comes and σ_{DT} is the time resolution of DT measurements, for which the measured value of 3 ns is used. The factor $(n-2)/n$ arises from computing measurement residuals in a plane and with respect to a straight line resulting from a fit to the same measurements. The weight for the i^{th} CSC measurement is given by:

$$w_i = \frac{L_i^2}{\sigma_i^2} \tag{6}$$

where σ_i, the measured time resolution, is 7.0 ns for cathode strip measurements and 8.6 ns for anode wire measurements.

To reduce the impact of outliers, which are mostly observed in the CSC anode wire measurement distribution, the CSC β^{-1} measurement whose difference with the track averaged β^{-1} is largest was discarded if the difference was greater than three times the estimated uncertainty ($\sigma_{\beta^{-1}}$) in the track averaged β^{-1}. The track averaged β^{-1} and the associated uncertainty were recomputed without the excluded measurement and the procedure was iterated until no further measurements could be discarded. A Gaussian fit to the core of the distribution of the β^{-1} measurements for the candidates passing the muon-like track pre-selection defined in Section 4 yielded a width of approximately 0.06, independent of the candidate pseudorapidity.

4 Trigger and data selection

Events were selected using a trigger requiring a muon with high transverse momentum ($p_T > 40\,\text{GeV}/c$) with $|\eta| < 2.1$, or a trigger requiring large missing transverse energy ($E_T^{miss} > 150$ GeV). The latter quantity was computed online using jets reconstructed with a particle-flow algorithm [53]. Jet clustering was performed using the anti-k_T algorithm [54] with a size parameter of 0.5. Triggering on E_T^{miss} allows the recovery of events with HSCPs failing muon identification or emerging mainly as neutral particles after traversing the calorimeters. The L1 muon trigger accepts tracks that produce signals in the RPC detectors either within the 25 ns time window corresponding to the collision bunch crossing, or within the following 25 ns time window. This operation mode is particularly suited for detecting late tracks in the muon system. It was designed to cater for this analysis, and is tenable as long as collisions are separated by 50 ns or more, which was the case for the 2011 LHC running period. The DT and CSC L1 triggers were used only for detecting particles produced in the collision bunch crossings. Track reconstruction in the muon HLT assumes particles traveling at the speed of light and produced within the triggered bunch crossing. However, the requirements on the quality of the muon segments are loose enough to allow tracks from late particles to be reconstructed with reasonably high efficiency. Events with pair produced $\widetilde{\tau}_1$, and with the fastest $\widetilde{\tau}_1$ having β as low as 0.6, would be selected by the muon trigger with 75% efficiency. The muon trigger efficiency would become less than 10% for events where the fastest $\widetilde{\tau}_1$ had $\beta \leq 0.45$.

The analysis made use of two offline selections referred to as 'tracker only' and 'tracker+TOF'. In the tracker-only selection, HSCP candidates were defined as individual tracks reconstructed in the inner tracker with large $\mathrm{d}E/\mathrm{d}x$ and p_T. In the tracker+TOF selection, the track was additionally required to be associated with an identified muon with long TOF. Events selected online with either of the muon or E_T^{miss} triggers were used in each of these two offline selections, to maximize the acceptance for HSCP signals. As described in section 6, the uncertainty in the signal acceptance arising from the uncertainty in the trigger efficiency is also reduced for some of the signals, because of the overlap of the two triggers. The tracker+TOF selection is not a subset of the tracker-only one because looser criteria on $\mathrm{d}E/\mathrm{d}x$ and p_T can be requested in the former.

For both offline selections, candidates were preselected by requiring p_T (as measured in the inner tracker) to be greater than $45\,\text{GeV}/c$, the relative uncertainty in the p_T to be smaller than 0.25, the track fit $\chi^2/\text{ndf} < 5$, $|\eta| < 1.5$, and the impact parameter $\sqrt{d_z^2 + d_{xy}^2} < 0.5\,\text{cm}$, where d_z and d_{xy} are the longitudinal and transverse impact parameters with respect to the reconstructed primary vertex that yields the smallest track d_z value. The η requirement results from a search optimization based on the best discovery reach, described in section 5. Candidates were required to have at least two measurements in the silicon pixel detectors and at least eleven measurements in the inner tracking detectors before the cleaning procedure. No more than 20% of the inner tracker layers were allowed to be missing between the first and last measurements of the track. Candidates were required to have at least six silicon strip measurements passing the cleaning procedure criteria and, therefore, used for the $\mathrm{d}E/\mathrm{d}x$ and mass measurements. Candidate tracks were required to have $I_h > 3\,\text{MeV}\,\text{cm}^{-1}$ for the initial selection. For the tracker+TOF candidates, the additional requirements of $\beta^{-1} > 1$, where β was computed from the TOF, and $\sigma_{\beta^{-1}} < 0.07$ were applied. The number of independent measurements used for the TOF computation was required to be greater than seven. Track candidates were required to be loosely isolated as measured by both the inner tracker and the calorimeters. Inner tracker isolation was established by considering all tracks whose direction had a distance from the candidate track direction, $\Delta R \equiv \sqrt{(\Delta\varphi)^2 + (\Delta\eta)^2} < 0.3$. The scalar sum of the p_T of these tracks,

with the exception of the candidate track, was required to be less than 50 (100) GeV/c for the tracker-only (tracker+TOF) selection. Calorimeter isolation was defined as the ratio between the sum of the energies measured in each ECAL and HCAL tower within a distance $\Delta R < 0.3$ from the candidate direction, and the candidate momentum. This ratio was required to be less than 0.3 (0.6) for the tracker-only (tracker+TOF) selection.

Good separation between HSCPs and SM particles may be achieved by selecting candidates with high p_{T}, high $\mathrm{d}E/\mathrm{d}x$, and long TOF (in the tracker+TOF selection). These quantities are expected to be uncorrelated for SM particles, while a slow-moving HSCP would have high $\mathrm{d}E/\mathrm{d}x$ and long TOF even at high p_{T}. Figure 1 shows the strong discrimination possible between simulated signals and background using I_{as}, TOF, and p_{T}. Because of the limited number of available simulated QCD multi-jet events with low transverse-momentum transfers, which contribute to the MC distributions for SM processes, these distributions display bin-to-bin variations in the size of the statistical errors. A disagreement was found in the tails of the I_{as} and β^{-1} distributions between the data and the simulation. The I_{as} discrepancy is understood as due to an increase with time of the average signal charge observed in the silicon strip detectors during the 2011 running period. These discrepancies in the tails have no impact on the estimated background rate since the latter is determined from data, as described in the following section. Signal acceptance is instead estimated from MC and studies were performed to assess the systematic uncertainty arising from the accuracy of the simulation model of I_{as} and TOF. They are detailed in section 6.

5 Background determination and search optimization

The search was performed as a counting experiment in a mass window that depended on the HSCP mass hypothesis, M, and the model of interest. For a given M, the mass window extended from $M_{\mathrm{reco}} - 2\sigma$ to 2 TeV/c^2, where M_{reco} is the average reconstructed mass for an HSCP of mass M and σ is the mass resolution expected at the true HSCP mass M. The values of M_{reco} and σ as a function of M were obtained from simulation.

The candidates passing the pre-selection described in Section 4 were used for both the signal search and background estimate. For the tracker-only selection, signal candidates were required to have I_{as} and p_{T} greater than threshold values optimized for each model and mass point, as described at the end of this section. A method that exploits the non-correlation between the p_{T} and $\mathrm{d}E/\mathrm{d}x$ measurements for SM particles was used to estimate the background. The number of candidates expected to pass both the final p_{T} and I_{as} thresholds was estimated as $D = BC/A$, where A is the number of candidates that fail both the I_{as} and p_{T} selections and B (C) is the number of candidates that pass only the I_{as} (p_{T}) selection. The B (C) candidates were then used to form a binned probability density function in I_{h} (p) for the D candidates such that, using the mass determination (Eq. (3)), the full mass spectrum of the background in the signal region D could be predicted. It was observed that the η distribution of the candidates at low $\mathrm{d}E/\mathrm{d}x$ differs from the distribution of the candidates at high $\mathrm{d}E/\mathrm{d}x$. This effect is due to the typical number of measurements attached to a track, which is η-dependent and is anticorrelated with both I_{as} and I_{h}. The η dependence of $\mathrm{d}E/\mathrm{d}x$ can bias the shape of the predicted background mass spectrum in the signal region because the p distribution is also η-dependent. To correct for this effect, events in the C region were weighted such that their η distribution matched that in the B region.

For the tracker+TOF selection, this method was extended to include the TOF measurement, assuming a lack of correlation between the TOF, p_{T}, and $\mathrm{d}E/\mathrm{d}x$ measurements. With three independent and uncorrelated variables, the number of background candidates in the signal

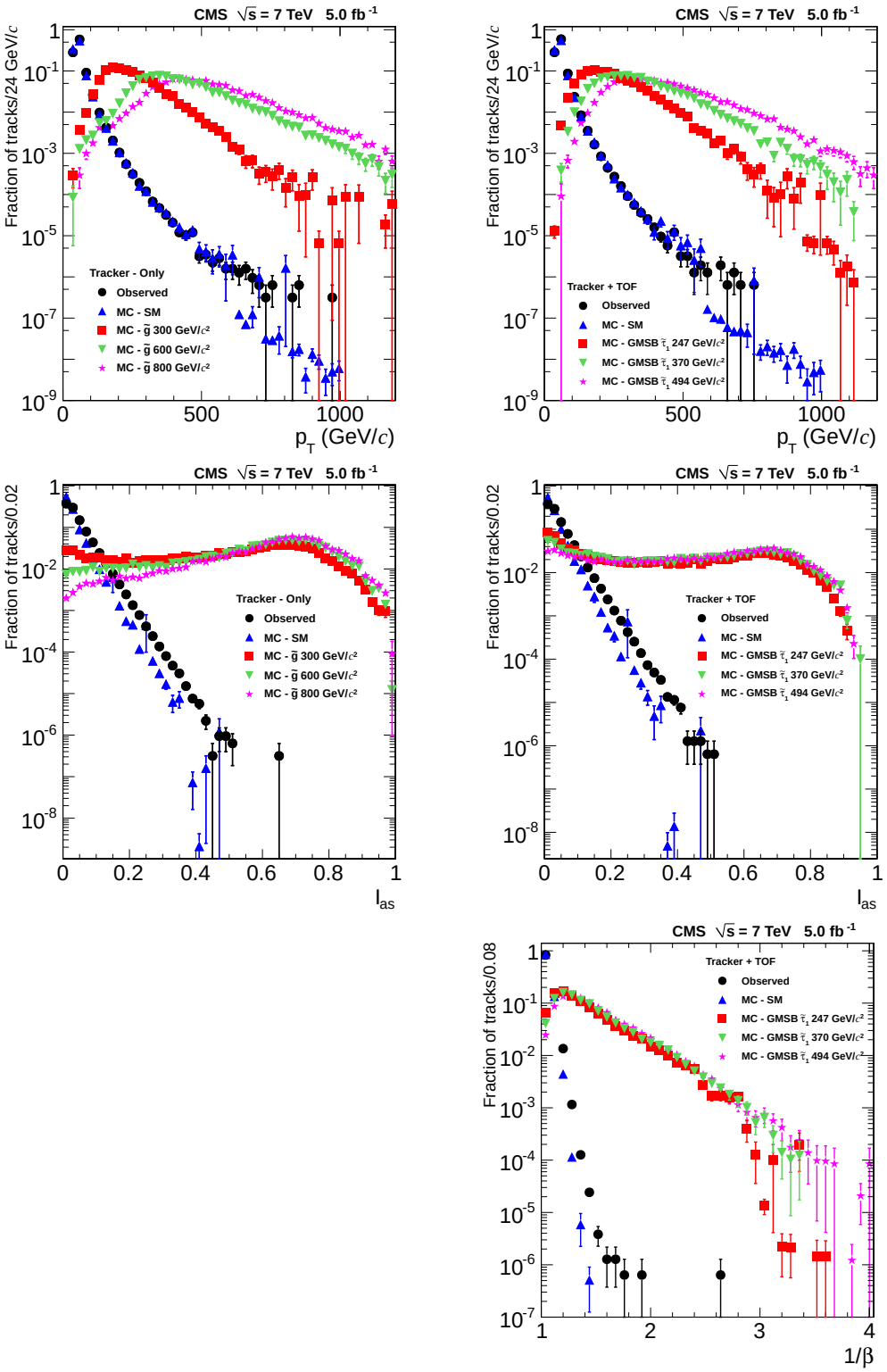

Figure 1: Normalized distributions of p_{T}, I_{as}, and β^{-1} in data, simulated SM processes, and some of the simulated signal samples. The two plots on the left are for the tracker-only selection. The three plots on the right are for the tracker+TOF selection. Different simulated signal samples are used for the left and right plots.

region may be estimated using six independent combinations of three out of the eight exclusive samples, each characterized by candidates passing or failing the three thresholds. These eight samples are analogous to the A, B, C, and D samples defined above. An additional independent background estimation in the signal region D may be obtained with a combination of four out of the eight samples. The corresponding expression is $D = AGF/E^2$, where E is the number of candidates that fail all selections, and A, G and F are the numbers of candidates that pass only the I_{as}, p_T, and TOF selection, respectively. This latter estimation has the smallest statistical uncertainty since the four samples are such that at most one of the three thresholds is passed in each of them, while the other estimations have at least one suppressed population sample because of the requirement for two thresholds to be exceeded. For this reason the background estimation was taken from this combination. As in the tracker-only analysis, weights were applied to correct the η distribution in the regions providing the $\mathrm{d}E/\mathrm{d}x$ and TOF binned probability density functions that were used to model the background from SM particles in the signal region. The dependence of the TOF measurement on η for genuine relativistic muons is due to differences in the typical number of track measurements, the accuracy of the measurements, the incident angles of particles on the detectors, and the residual magnetic field in the muon chamber drift volumes. The systematic uncertainty in the expected background in the signal region is estimated to be 10%, from the differences observed between the four background estimates having the smallest statistical uncertainties. The same uncertainty was adopted for the tracker-only selection. The statistical uncertainty of the background estimation in either the whole signal region or in a given mass range was obtained by generating simulated pseudoexperiments drawn from the observed distributions in the control regions.

A 'loose' selection is defined such that there are a relatively large number of background candidates in the signal region. This selection allows a cross-check on the accuracy of the background prediction to be performed. Table 1 reports the minimum values of p_T, I_{as}, and β^{-1} that candidates must have to pass this selection, as well as the absolute yields of the background prediction and the observed data. Figure 2 shows agreement between the observed and predicted mass spectra obtained using the loose selection for both the tracker-only and tracker+TOF candidates. The background prediction obtained from simulation using the same method as for data is shown in the same figure.

Table 1: Selections used to create the 'loose' samples with large number of events and the expected (Exp.) and observed (Obs.) event yields. The selections are defined in terms of thresholds in p_T, I_{as}, and β^{-1} (measured from TOF).

Selection	p_T^{min} (GeV/c)	I_{as}^{min}	β^{-1min}	Exp.	Obs.
Tk-Only	50	0.10	-	103450 $\pm$ 10350 (syst) $\pm$ 210 (stat)	94910
Tk+TOF	50	0.05	1.05	88010 $\pm$ 8800 (syst) $\pm$ 290 (stat)	72079

The final selection thresholds on p_T, I_{as}, and TOF were optimized for each signal model and mass by minimizing the signal cross section value for which a discovery would be achieved, where discovery is defined as the expected mean significance of the observed excess being equal to five standard deviations with at least five observed candidates. It was verified that in all cases the optimized thresholds also guarantee that the expected 95% confidence level (CL) cross section upper limit on the considered model is at most 10% larger than the minimum attainable. The optimized selection thresholds and the resulting signal acceptance for some representative signal models are reported in Tables 2 and 3.

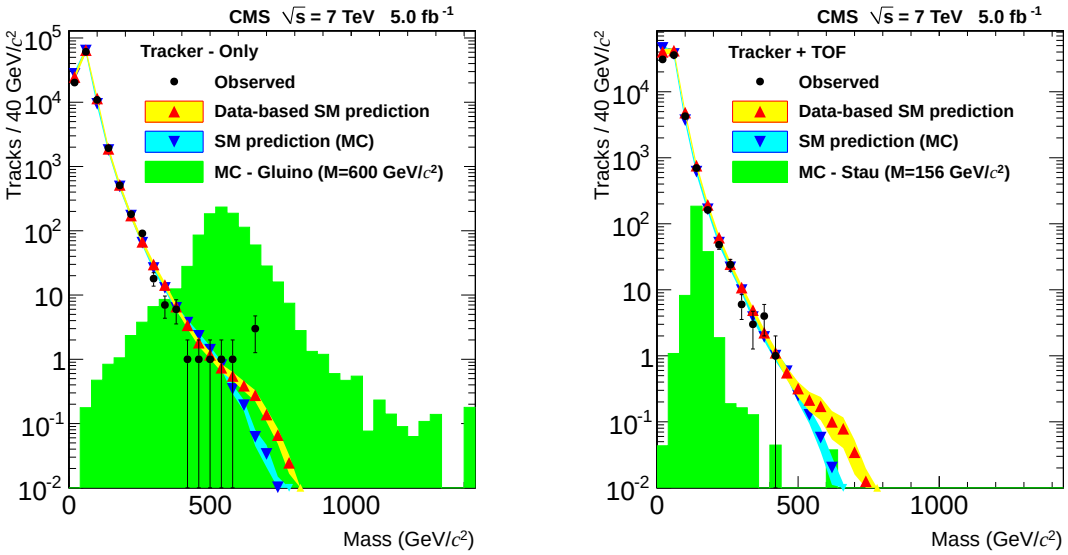

Figure 2: Distribution of the candidate mass for the loose selection defined in Table 1, for the tracker-only (left) and tracker+TOF (right) candidates. Shown are: data, background estimate from data with its uncertainty (yellow band), simulated signal (green shaded histogram) and background prediction from MC (blue band) using the same method as for data.

Table 2: Results of the tracker-only analysis for some representative signal mass values (in GeV/c^2): final selections in terms of minimum values of p_T (in GeV/c), I_{as}, β^{-1}, and M_{reco} (in GeV/c^2), signal acceptance ("Acc"), number of candidates expected from SM background ("Exp."), number of observed candidates ("Obs."), predicted theoretical cross section ("Th. σ"), expected median cross section upper limit at 95% CL for the background-only hypothesis ("Exp. σ"), and observed 95% CL cross section upper limit ("Obs. σ"). All cross section values are expressed in pb.

Model	Mass	p_T^{min}	I_{as}^{min}	M_{reco}^{min}	Acc.	Exp.	Obs.	Th. σ	Exp. σ	Obs. σ
$\tilde{g}$ ($f = 0.1$)	300	60	0.400	180	0.16	0.328 ± 0.040	0	6.6E+01	3.8E-03	3.7E-03
$\tilde{g}$ ($f = 0.1$)	700	50	0.300	410	0.21	0.089 ± 0.009	1	2.1E-01	3.0E-03	4.0E-03
$\tilde{g}$ ($f = 0.1$)	1100	120	0.225	570	0.15	0.094 ± 0.010	0	3.9E-03	4.0E-03	3.9E-03
$\tilde{g}$ ($f = 0.5$)	300	60	0.400	180	0.086	0.328 ± 0.040	0	6.6E+01	6.9E-03	6.8E-03
$\tilde{g}$ ($f = 0.5$)	700	50	0.300	410	0.12	0.089 ± 0.009	1	2.1E-01	5.3E-03	7.1E-03
$\tilde{g}$ ($f = 0.5$)	1100	120	0.225	570	0.085	0.094 ± 0.010	0	3.9E-03	7.0E-03	6.9E-03
$\tilde{g}$ ($f = 0.1$, ch. suppr.)	300	60	0.400	180	0.020	0.328 ± 0.040	0	6.6E+01	3.0E-02	3.0E-02
$\tilde{g}$ ($f = 0.1$, ch. suppr.)	700	50	0.325	370	0.045	0.092 ± 0.010	1	2.1E-01	1.4E-02	1.8E-02
$\tilde{g}$ ($f = 0.1$, ch. suppr.)	1100	50	0.275	460	0.032	0.085 ± 0.009	1	3.9E-03	1.9E-02	2.6E-02
$\tilde{t}_1$	200	60	0.400	130	0.14	1.250 ± 0.160	4	1.3E+01	5.8E-03	1.1E-02
$\tilde{t}_1$	500	50	0.350	310	0.24	0.126 ± 0.014	0	4.8E-02	2.4E-03	2.3E-03
$\tilde{t}_1$	800	50	0.275	450	0.29	0.095 ± 0.010	1	1.1E-03	2.1E-03	2.8E-03
$\tilde{t}_1$ (ch. suppr.)	200	70	0.400	120	0.021	1.520 ± 0.202	4	1.3E+01	4.0E-02	7.2E-02
$\tilde{t}_1$ (ch. suppr.)	500	50	0.375	280	0.064	0.102 ± 0.012	0	4.8E-02	9.1E-03	9.1E-03
$\tilde{t}_1$ (ch. suppr.)	800	50	0.325	370	0.077	0.092 ± 0.010	1	1.1E-03	8.1E-03	1.1E-02
GMSB $\tilde{\tau}_1$	100	65	0.400	20	0.12	6.980 ± 0.908	7	1.3E+00	1.2E-02	1.3E-02
GMSB $\tilde{\tau}_1$	494	65	0.350	300	0.64	0.126 ± 0.014	0	6.2E-05	9.3E-04	9.3E-04
pair prod. $\tilde{\tau}_1$	100	70	0.400	40	0.11	4.840 ± 0.608	6	3.8E-02	1.2E-02	1.5E-02
pair prod. $\tilde{\tau}_1$	308	70	0.400	190	0.39	0.237 ± 0.030	0	3.5E-04	1.5E-03	1.5E-03
$\widetilde{K}$ ($\bar{\rho}$ (800))	100	70	0.400	10	0.065	4.880 ± 0.613	6	1.4E+00	1.9E-02	2.3E-02
$\widetilde{K}$ ($\bar{\rho}$ (800))	500	50	0.350	320	0.61	0.107 ± 0.012	0	2.8E-04	9.6E-04	9.6E-04
$\widetilde{K}$ ($\bar{\rho}$ (1200))	600	50	0.325	370	0.22	0.092 ± 0.010	1	2.6E-03	2.8E-03	3.8E-03
$\widetilde{K}$ ($\bar{\rho}$ (1200))	700	50	0.275	440	0.65	0.106 ± 0.011	1	6.1E-05	9.6E-04	1.3E-03
$\widetilde{K}$ ($\bar{\rho}$ (1600))	800	140	0.250	480	0.33	0.118 ± 0.012	1	2.6E-04	1.9E-03	2.5E-03
$\widetilde{K}$ ($\bar{\rho}$ (1600))	900	135	0.225	530	0.62	0.128 ± 0.014	0	1.3E-05	9.3E-04	9.3E-04

Table 3: Results of the tracker+TOF analysis for some representative signal mass values (in GeV/c^2): final selections in terms of minimum values of p_T (in GeV/c), I_{as}, β^{-1}, and M_{reco} (in GeV/c^2), signal acceptance ("Acc"), number of candidates expected from SM background ("Exp."), number of observed candidates ("Obs."), predicted theoretical cross section ("Th. σ"), expected median cross section upper limit at 95% CL for the background-only hypothesis ("Exp. σ"), and observed 95% CL cross section upper limit ("Obs. σ"). All cross section values are expressed in pb.

Model	Mass	p_T^{min}	I_{as}^{min}	β^{-1min}	M_{eco}^{min}	Acc.	Exp.	Obs.	Th. σ	Exp. σ	Obs. σ
$\widetilde{g}$ ($f = 0.1$)	300	55	0.175	1.175	180	0.17	0.119 ± 0.012	0	6.6E+01	3.4E-03	3.4E-03
$\widetilde{g}$ ($f = 0.1$)	700	110	0.050	1.125	430	0.19	0.113 ± 0.015	0	2.1E-01	3.0E-03	3.0E-03
$\widetilde{g}$ ($f = 0.1$)	1100	110	0.025	1.075	620	0.13	0.111 ± 0.033	0	3.9E-03	4.6E-03	4.6E-03
$\widetilde{g}$ ($f = 0.5$)	300	55	0.175	1.175	180	0.094	0.119 ± 0.012	0	6.6E+01	6.3E-03	6.2E-03
$\widetilde{g}$ ($f = 0.5$)	700	110	0.050	1.125	430	0.11	0.113 ± 0.015	0	2.1E-01	5.4E-03	5.3E-03
$\widetilde{g}$ ($f = 0.5$)	1100	110	0.025	1.075	620	0.072	0.111 ± 0.033	0	3.9E-03	8.2E-03	8.2E-03
$\widetilde{t}_1$	200	50	0.200	1.200	130	0.15	0.109 ± 0.011	0	1.3E+01	3.9E-03	3.8E-03
$\widetilde{t}_1$	500	60	0.075	1.150	330	0.25	0.125 ± 0.013	0	4.8E-02	2.4E-03	2.4E-03
$\widetilde{t}_1$	800	105	0.025	1.125	490	0.26	0.096 ± 0.019	0	1.1E-03	2.2E-03	2.2E-03
GMSB $\widetilde{\tau}_1$	100	50	0.300	1.275	30	0.20	0.093 ± 0.011	0	1.3E+00	2.9E-03	2.9E-03
GMSB $\widetilde{\tau}_1$	494	55	0.025	1.175	320	0.78	0.113 ± 0.014	1	6.2E-05	7.8E-04	1.1E-03
pair prod. $\widetilde{\tau}_1$	100	50	0.250	1.275	50	0.19	0.109 ± 0.012	0	3.8E-02	3.0E-03	2.9E-03
pair prod. $\widetilde{\tau}_1$	308	65	0.125	1.200	190	0.55	0.105 ± 0.011	0	3.5E-04	1.1E-03	1.1E-03
$\widetilde{K}$ ($\widetilde{\rho}$ (800))	100	50	0.300	1.275	20	0.11	0.095 ± 0.011	0	1.4E+00	5.3E-03	5.2E-03
$\widetilde{K}$ ($\widetilde{\rho}$ (800))	500	60	0.075	1.150	330	0.68	0.125 ± 0.013	0	2.8E-04	8.6E-04	8.5E-04
$\widetilde{K}$ ($\widetilde{\rho}$ (1200))	600	70	0.025	1.150	380	0.22	0.107 ± 0.015	0	2.6E-03	2.6E-03	2.6E-03
$\widetilde{K}$ ($\widetilde{\rho}$ (1200))	700	110	0.050	1.125	450	0.66	0.087 ± 0.013	0	6.1E-05	9.0E-04	9.0E-04
$\widetilde{K}$ ($\widetilde{\rho}$ (1600))	800	50	0.050	1.100	500	0.33	0.119 ± 0.021	0	2.6E-04	1.8E-03	1.8E-03
$\widetilde{K}$ ($\widetilde{\rho}$ (1600))	900	85	0.075	1.075	550	0.61	0.123 ± 0.022	0	1.3E-05	9.3E-04	9.1E-04

6 Results

After comparing data in the signal region with the expected background for all optimized selections, no statistically significant excess was observed. Tables 2 and 3 report results for some representative selections. The largest excess has a significance of 1.75 one-sided Gaussian standard deviations and was found with the selection optimized for a $\widetilde{t}_1$ with a mass of 200 GeV/c^2. Only one of the three highest mass candidates passing the tracker-only loose selection (Fig. 2) passes one of the final selections. This candidate is also associated with an identified muon and has $\beta^{-1} = 1.03$, which is well below any threshold used in the tracker+TOF final selections.

The observed data sample was used to calculate upper limits on the HSCP production cross section for each considered model and mass point. The cross section upper limits at 95% CL were obtained using a CL_s approach [55] with a one-sided profile likelihood test statistic whose p-values were evaluated by generating pseudoexperiments using a frequentist prescription [56]. A log-normal probability density function [50] was used for the nuisance parameter measurements, which are the integrated luminosity, the signal acceptance, and the expected background yield in the signal region. When generating pseudoexperiments for the limit calculation, each nuisance parameter was drawn from the corresponding probability density function with a central value equal to the best fit value to data under the signal+background hypothesis. All systematic uncertainties are summarized in Table 4 and are incorporated in the limits quoted below.

Simulation was used to determine the signal acceptance. A number of studies were undertaken to estimate the degree to which the simulation correctly models the detector response to HSCPs and to assess an uncertainty in the signal acceptance.

The uncertainty in the trigger efficiency derived from simulation was evaluated separately for the E_T^{miss} and single-muon triggers. The uncertainty in the E_T^{miss} trigger efficiency was domi-

nated by the uncertainty in the jet-energy scale [57], which was less than 3% across the energy range. For the charge-suppression models, where the $E_{\mathrm{T}}^{\mathrm{miss}}$ trigger is most relevant, varying the jet-energy scale and jet-energy resolution within their uncertainty resulted in a relative change of the trigger efficiency by no more than 5%. For all the other models, which made use of overlap with the single-muon trigger, the relative change of the overall trigger efficiency was found to vary by no more than 2%. For the single-muon trigger, a relative disagreement of up to 5% was observed between the efficiency estimated in data and MC at all energies [58]. In addition, for this specific analysis, a further uncertainty arises from the imperfect simulation of the synchronization of the muon trigger electronics. The accuracy of the synchronization was evaluated from data separately for each muon subdetector. This effect was found to yield less than 2% relative uncertainty on the overall trigger efficiency for all considered signals. On the basis of these numbers, an uncertainty of 5% on the overall trigger efficiency was assumed for all models.

The accuracy of the $\mathrm{d}E/\mathrm{d}x$ model used in simulation was studied using low-momentum protons and kaons. The simulation was found to underestimate both the I_{h} and I_{as} scales by less than 5%. The I_{as} resolution was in contrast found to be overestimated by a constant value of 0.08 in the region around the thresholds adopted in the analysis. After corrections for these discrepancies were applied to simulation, only 20% of the signal models displayed an efficiency decrease, with the maximum relative reduction being smaller than 2%. The efficiency for all other models increased by up to 10% relative to the uncorrected MC result. Based on these results, the efficiency determined from the simulation was not corrected, but was assigned an associated uncertainty of 2%.

The accuracy of the TOF model implemented in the simulation was studied using cosmic ray muons and muons produced directly in collisions. In the region around the β^{-1} thresholds adopted in the analysis, the simulation was found to overestimate β^{-1} by a constant value of 0.003 and 0.02 for DT and CSC, respectively. The resolution of the measurement of β^{-1} was found to be well modelled in simulation. After corrections for these discrepancies were applied, the signal efficiency was found to decrease by no more than 2% for all considered models and mass points. This maximum change of 2% was adopted as the uncertainty associated with the TOF measurement.

The uncertainty on the track momentum scale was modelled by varying the track p_{T} as a function of the track ϕ and η values such that [59]:

$$\frac{1}{p'_{\mathrm{T}}} = \frac{1}{p_{\mathrm{T}}} + \delta_{K_T}(q, \phi, \eta), \tag{7}$$

$$\delta_{K_T}(q, \phi, \eta) = a + b\eta^2 + qd\sin(\phi - \phi_0), \tag{8}$$

where q is the track charge sign ($q = \pm 1$) and the function δ_{K_T} controls the shift in the track momentum scale. This function has four free parameters, a, b, d, and ϕ_0, whose values were obtained [59] by minimizing the difference between the invariant mass distributions of $Z \to \mu^+\mu^-$ candidates in data and simulation. The obtained values are $a = 0.236\,\mathrm{TeV}^{-1}c$, $b = -0.135\,\mathrm{TeV}^{-1}c$, $d = 0.282\,\mathrm{TeV}^{-1}c$, and $\phi_0 = 1.337$ rad. The phi dependence is believed to be due to imperfect inner tracker alignment. The expected shift in inverse p_{T} for tracks of higher momenta measured in the inner tracker are found [59] to be compatible with those provided by equations 7 and 8. The difference between the signal acceptance with the nominal and shifted p_{T} was taken as the uncertainty and was found to be smaller than 4%.

Table 4: Sources of systematic uncertainties and corresponding relative uncertainties.

Source of systematic uncert.	Relative uncert. (%)
Signal acceptance:	
- Trigger efficiency	5
- Track momentum scale	< 4
- Ionization energy loss	2
- Time-of-flight	2
- Track reconstruction eff.	< 2
- Muon reconstruction eff.	< 2
- Pile-up	< 0.5
Total uncert. in signal acc.	7
Expected background	10
Integrated luminosity	2.2

The uncertainties in the efficiencies for reconstructing muons [58], and for reconstructing tracks in the inner tracker [60] were also considered and established to be less than 2% in each case.

The impact of the uncertainty in the mean rate of additional interactions in each bunch crossing was studied and found to be negligible compared to the statistical precision (0.5%) allowed by the size of the simulated signal samples.

Two theoretical uncertainties affecting the signal acceptance were studied: the uncertainty in the model of hadronization and nuclear interactions, and the uncertainty due to the MPI tune. The hadronization and nuclear-interaction model is discussed in Section 2. Results are obtained for two very different nuclear interaction models and for two different $\tilde{g}$ hadronization schemes. With regard to the MPI tune, tune Z2 uses a p_T-ordered model, which appears to generate significantly more initial-state radiation than the Q^2-ordered D6T model. For some models a significant increase in the trigger efficiency and in the reconstruction efficiency is found and the observed limits become more stringent. The most conservative set of limits, resulting from the Q^2-ordered D6T model, are those reported.

An uncertainty of 2.2% is estimated [61] for the absolute value of the integrated luminosity. The uncertainty in the expected background was discussed in Section 5 and is estimated to be of the order of 10%. This uncertainty has very little impact on the results, because of the small numbers of expected events for most mass points.

The 95% CL cross section upper limit curves obtained with both the tracker-only and the tracker+TOF selection are shown in Figs. 3 and 4, along with the theoretical predictions for the chosen signal models. The ratio of observed to expected 95% CL upper limits on the cross section is reported in Fig. 5 for the different combinations of models and scenarios considered. Numerical values for the predicted theoretical cross section, and expected and observed cross section upper limit at 95% CL are reported in Tables 2 and 3 for some representative signal models. For $\widetilde{t}_1$ and $\tilde{g}$ pair production, theoretical cross sections were computed at next-to-leading order (NLO) plus next-to-leading-logarithmic (NLL) accuracy [62–66] using PROSPINO v2.1 [67]. The uncertainty in these theoretical cross section values varies between 10% to 25% and is shown in Fig. 3 as a band around the central value. The cross sections for the models with $\widetilde{\tau}_1$ production were calculated at NLO with PROSPINO v2.1. The uncertainty in the theoretical cross section was estimated to be 5% to 14% for the GMSB model and 3% to 7% for direct $\widetilde{\tau}_1$ pair production, depending on the mass. In all cases the sources of uncertainty include renormalization and factorization scales, α_s, and the parton distribution functions. The cross sections for $\widetilde{K}$

production used in this paper are computed at leading order only. The theoretical uncertainty was not evaluated because of the lack of corresponding theoretical NLO calculations. For a fixed $\widetilde{\rho}$ mass, the $\widetilde{\mathrm{K}}\,\overline{\widetilde{\mathrm{K}}}$ cross section is a combination of a $\widetilde{\rho}$ resonance and Drell-Yan production. When the $\widetilde{\mathrm{K}}$ mass is much smaller than half the $\widetilde{\rho}$ mass, Drell-Yan production dominates. As the $\widetilde{\mathrm{K}}$ mass increases, resonance production becomes increasingly important, and dominates as the kinematic limit for $\widetilde{\mathrm{K}}\,\overline{\widetilde{\mathrm{K}}}$ pair production is approached. For $\widetilde{\mathrm{K}}$ mass greater than half the $\widetilde{\rho}$ mass, resonance production turns off, resulting in a steep drop in the total cross section (shown by the nearly vertical line in Fig. 4). In addition, near the kinematic limit the $\widetilde{\rho} \to \widetilde{\mathrm{K}}\,\overline{\widetilde{\mathrm{K}}}$ process produces very low velocity $\widetilde{\mathrm{K}}$ particles. The signal acceptance therefore decreases dramatically until the resonance production turns off, at which point the acceptance increases again. This results in a spike in the cross section limit near the kinematic limit.

From the intersection of the cross section limit curve and the central value of the theoretical cross section band, a 95% CL lower limit of 1098 (1046) GeV/c^2 on the mass of pair produced $\widetilde{\mathrm{g}}$, hadronizing into stable R-gluonballs with 0.1 (0.5) probability, is determined with the tracker-only selection. The tracker+TOF selection gives a lower limit of 1082 (1030) GeV/c^2 for the same signal model. The analogous limit on the $\widetilde{\mathrm{t}}_1$ mass is 714 GeV/c^2 with the tracker-only selection and 737 GeV/c^2 with the tracker+TOF selection. The charge suppression scenario discussed above yields a $\widetilde{\mathrm{g}}$ mass limit of 928 GeV/c^2 for $f = 0.1$ and 626 GeV/c^2 for the $\widetilde{\mathrm{t}}_1$. The limits on GMSB and pair produced $\widetilde{\tau}_1$ are calculated at 314 and 223 GeV/c^2, respectively, with the tracker+TOF selection. The mass limits on $\widetilde{\mathrm{K}}$ are established at 484, 602 and 747 GeV/c^2 for $\widetilde{\rho}$ masses of 800, 1200 and 1600 GeV/c^2, respectively, with the tracker+TOF selection.

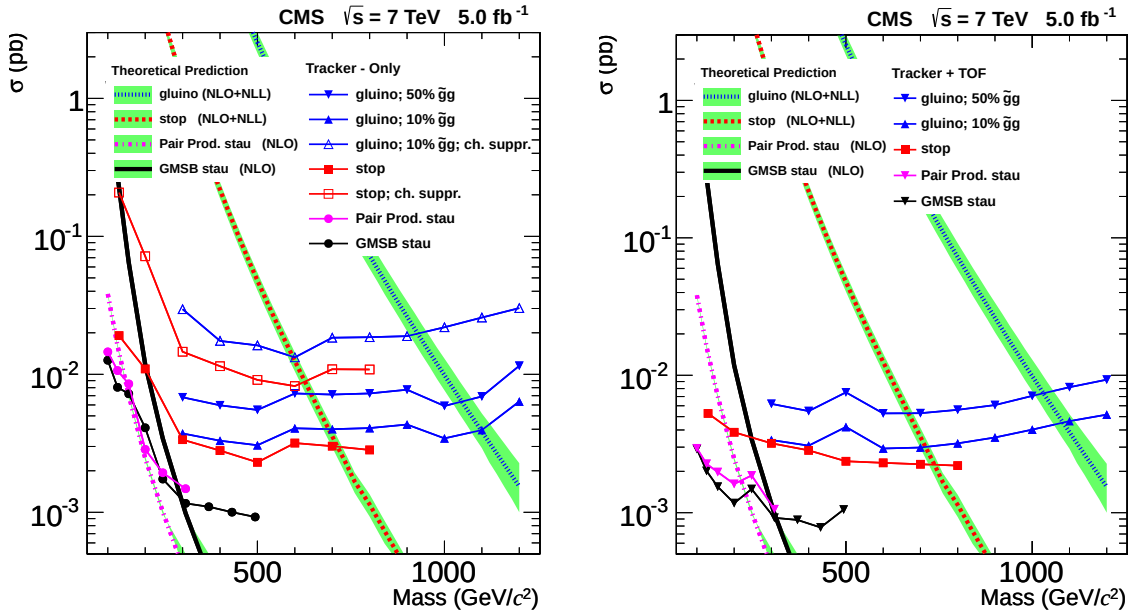

Figure 3: Predicted theoretical cross section and observed 95% CL upper limits on the cross section for the different signal models considered: production of $\widetilde{\mathrm{t}}_1$, $\widetilde{\mathrm{g}}$, and $\widetilde{\tau}_1$; different fractions f of R-gluonball states produced after hadronization; standard and charge suppression (ch. suppr.) scenario. Left: tracker-only selection. Right: tracker+TOF. The uncertainties in the theoretical cross section are shown as bands around the central values.

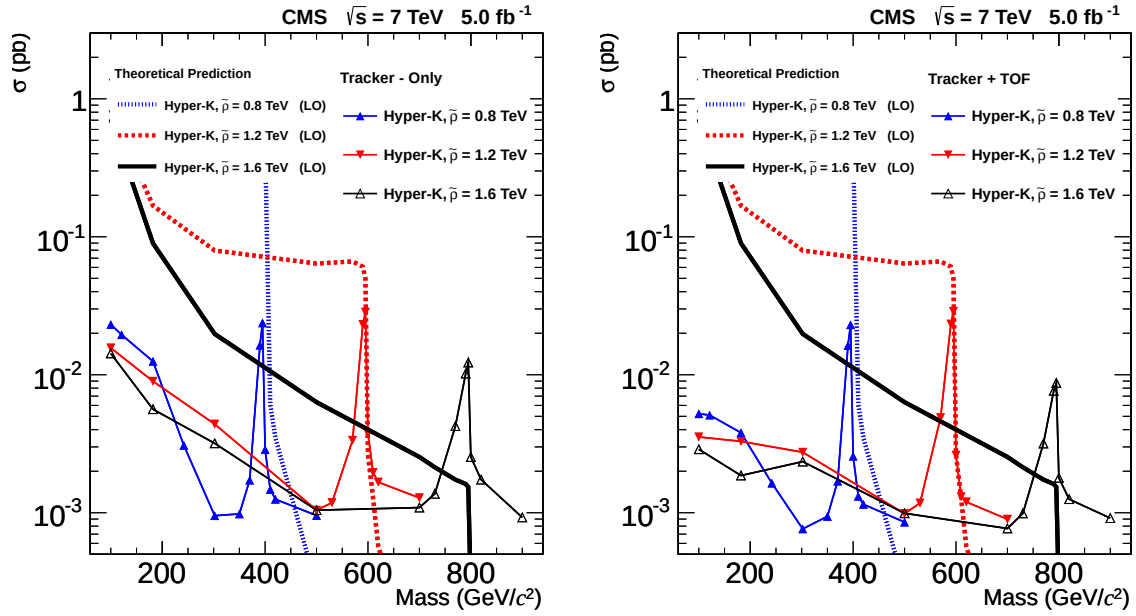

Figure 4: Predicted theoretical cross section and observed 95% CL upper limits on the cross section for the $\widetilde{\mathrm{K}}$ models with different $\tilde{\rho}$ mass values. Left: tracker-only selection. Right: tracker+TOF.

7 Summary

The CMS detector has been used to search for highly ionizing, high-p_{T} and long time-of-flight massive particles. Two inclusive searches have been conducted: one that uses highly ionizing tracks reconstructed in the inner tracker, and a second requiring that these tracks also be identified in the CMS muon system and have long time-of-flight. The former is model-independent in that it is insensitive to the details of R-hadron nuclear interactions. In each case, the observed number of candidates is consistent with the expected background. Upper limits on production cross section and lower limits on masses of stable, weakly- and strongly-interacting particles have been established for a variety of models. They range from 223 GeV/c^2 for a pair produced scalar tau to 1098 GeV/c^2 for a pair-produced gluino. These limits are the most restrictive to date.

8 Acknowledgements

We congratulate our colleagues in the CERN accelerator departments for the excellent performance of the LHC machine. We thank the technical and administrative staff at CERN and other CMS institutes, and acknowledge support from: FMSR (Austria); FNRS and FWO (Belgium); CNPq, CAPES, FAPERJ, and FAPESP (Brazil); MES (Bulgaria); CERN; CAS, MoST, and NSFC (China); COLCIENCIAS (Colombia); MSES (Croatia); RPF (Cyprus); MoER, SF0690030s09 and ERDF (Estonia); Academy of Finland, MEC, and HIP (Finland); CEA and CNRS/IN2P3 (France); BMBF, DFG, and HGF (Germany); GSRT (Greece); OTKA and NKTH (Hungary); DAE and DST (India); IPM (Iran); SFI (Ireland); INFN (Italy); NRF and WCU (Korea); LAS (Lithuania); CINVESTAV, CONACYT, SEP, and UASLP-FAI (Mexico); MSI (New Zealand); PAEC (Pakistan); MSHE and NSC (Poland); FCT (Portugal); JINR (Armenia, Belarus, Georgia, Ukraine, Uzbekistan); MON, RosAtom, RAS and RFBR (Russia); MSTD (Serbia); MICINN and CPAN (Spain); Swiss Funding Agencies (Switzerland); NSC (Taipei); TUBITAK and TAEK (Turkey); STFC

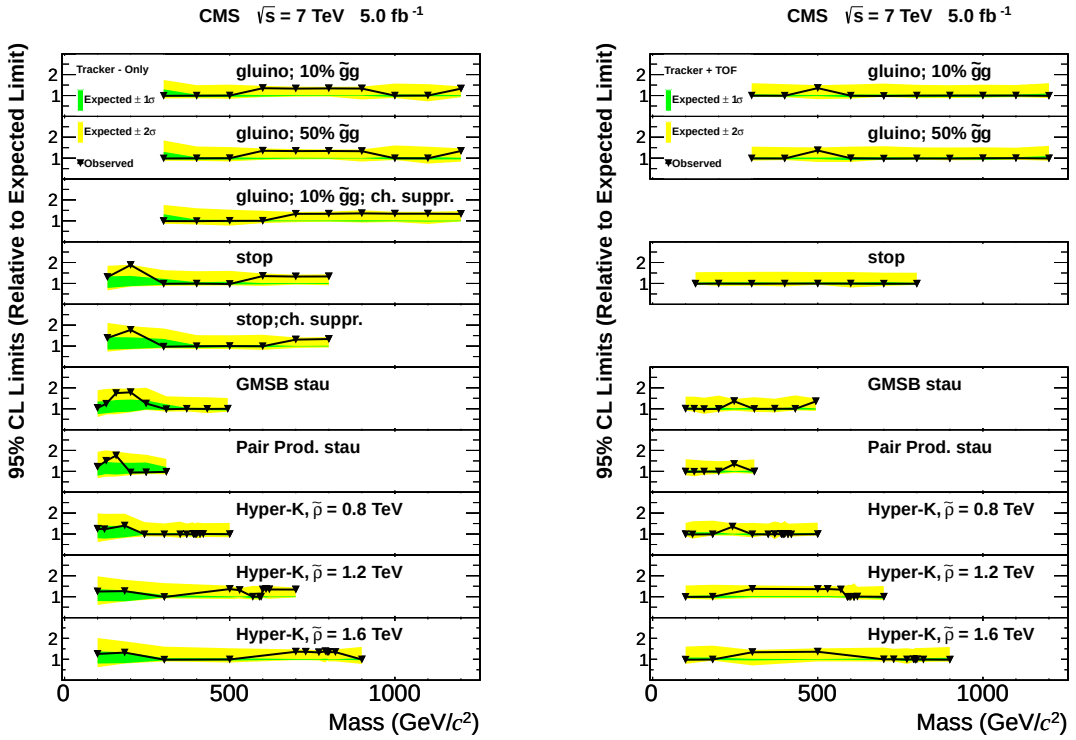

Figure 5: Ratio of observed 95% CL upper limits to expected median limits for the background-only hypothesis. The green (dark) and yellow (light) bands indicate the ranges that are expected to contain 68% and 95% of all observed excursions from the expected median, respectively. Ratios are presented for the different signal models considered: production of $\widetilde{g}$, $\widetilde{t}_1$, $\widetilde{\tau}_1$, and $\widetilde{K}$; different fractions, f, of R-gluonball states produced after hadronization; standard or charge suppression (ch. suppr.) scenario. Left: tracker-only selection. Right: tracker+TOF.

(United Kingdom); DOE and NSF (USA).

Individuals have received support from the Marie-Curie programme and the European Research Council (European Union); the Leventis Foundation; the A. P. Sloan Foundation; the Alexander von Humboldt Foundation; the Belgian Federal Science Policy Office; the Fonds pour la Formation à la Recherche dans l'Industrie et dans l'Agriculture (FRIA-Belgium); the Agentschap voor Innovatie door Wetenschap en Technologie (IWT-Belgium); the Council of Science and Industrial Research, India; and the HOMING PLUS programme of Foundation for Polish Science, cofinanced from European Union, Regional Development Fund.

References

[1] M. Drees and X. Tata, "Signals for heavy exotics at hadron colliders and supercolliders", *Phys. Lett. B* **252** (1990) 695–702, doi:10.1016/0370-2693(90)90508-4.

[2] M. Fairbairn et al., "Stable massive particles at colliders", *Phys. Rept.* **438** (2007) 1–63, doi:10.1016/j.physrep.2006.10.002, arXiv:hep-ph/0611040.

[3] C. W. Bauer et al., "Supermodels for early LHC", *Phys. Lett. B* **690** (2010) 280–288, doi:10.1016/j.physletb.2010.05.032, arXiv:0909.5213.

[4] ALEPH Collaboration, "Search for pair production of longlived heavy charged particles in e+ e- annihilation", *Phys. Lett. B* **405** (1997) 379–388, doi:10.1016/S0370-2693(97)00715-6, arXiv:hep-ex/9706013.

[5] DELPHI Collaboration, "Search for heavy stable and longlived particles in e+ e- collisions at $\sqrt{s} = 189$ GeV", *Phys. Lett. B* **478** (2000) 65–72, doi:10.1016/S0370-2693(00)00265-3, arXiv:hep-ex/0103038.

[6] L3 Collaboration, "Search for heavy neutral and charged leptons in e^+e^- annihilation at LEP", *Phys. Lett. B* **517** (2001) 75–85, doi:10.1016/S0370-2693(01)01005-X, arXiv:hep-ex/0107015.

[7] OPAL Collaboration, "Search for stable and longlived massive charged particles in e+ e- collisions at $\sqrt{s} = 130$ GeV to 209 GeV", *Phys. Lett. B* **572** (2003) 8–20, doi:10.1016/S0370-2693(03)00639-7, arXiv:hep-ex/0305031.

[8] H1 Collaboration, "Measurement of anti-deuteron photoproduction and a search for heavy stable charged particles at HERA", *Eur. Phys. J. C* **36** (2004) 413–423, doi:10.1140/epjc/s2004-01894-1, arXiv:hep-ex/0403056.

[9] CDF Collaboration, "Search for Heavy Stable Particles at the Fermilab Collider", *Phys. Rev. Lett.* **63** (1989) 1447, doi:10.1103/PhysRevLett.63.1447.

[10] CDF Collaboration, "Limits on the production of massive stable charged particles", *Phys. Rev. D* **46** (1992) 1889–1894, doi:10.1103/PhysRevD.46.R1889.

[11] CDF Collaboration, "Search for long-lived charged massive particles in $\bar{p}p$ collisions at $\sqrt{s} = 1.8$ TeV", *Phys. Rev. Lett.* **90** (2003) 131801, doi:10.1103/PhysRevLett.90.131801, arXiv:hep-ex/0211064.

[12] D0 Collaboration, "Search for stopped gluinos from $p\bar{p}$ collisions at $\sqrt{s} = 1.96$ TeV", *Phys. Rev. Lett.* **99** (2007) 131801, doi:10.1103/PhysRevLett.99.131801, arXiv:0705.0306.

[13] D0 Collaboration, "Search for Long-Lived Charged Massive Particles with the D0 Detector", *Phys. Rev. Lett.* **102** (2009) 161802, doi:10.1103/PhysRevLett.102.161802, arXiv:0809.4472.

[14] CDF Collaboration, "Search for Long-Lived Massive Charged Particles in 1.96 TeV $\bar{p}p$ Collisions", *Phys. Rev. Lett.* **103** (2009) 021802, doi:10.1103/PhysRevLett.103.021802, arXiv:0902.1266.

[15] D0 Collaboration, "Search for Charged Massive Long-Lived Particles", *Phys. Rev. Lett.* **108** (2012) 121802, doi:10.1103/PhysRevLett.108.121802.

[16] CMS Collaboration, "Search for Stopped Gluinos in pp Collisions at $\sqrt{s} = 7$ *TeV*", *Phys. Rev. Lett.* **106** (2011) 011801, doi:10.1103/PhysRevLett.106.011801, arXiv:1011.5861.

[17] CMS Collaboration, "Search for heavy stable charged particles in pp collisions at $\sqrt{s} = 7$ TeV", *JHEP* **03** (2011) 024, doi:10.1007/JHEP03(2011)024, arXiv:1101.1645.

[18] ATLAS Collaboration, "Search for massive long-lived highly ionising particles with the ATLAS detector at the LHC", *Phys. Lett. B* **698** (2011) 353–370, doi:10.1016/j.physletb.2011.03.033, arXiv:1102.0459.

[19] ATLAS Collaboration, "Search for stable hadronising squarks and gluinos with the ATLAS experiment at the LHC", *Phys. Lett. B* **701** (2011) 1–19, doi:10.1016/j.physletb.2011.05.010, arXiv:1103.1984.

[20] ATLAS Collaboration, "Search for heavy long-lived charged particles with the ATLAS detector in pp collisions at $\sqrt{s} = 7$ TeV", *Phys. Lett. B* **703** (2011) 428–446, doi:10.1016/j.physletb.2011.08.042, arXiv:1106.4495.

[21] ATLAS Collaboration, "Search for decays of stopped, long-lived particles from 7 TeV pp collisions with the ATLAS detector", (2012). arXiv:1201.5595. Submitted to *Eur. Phys. J. C.*

[22] G. R. Farrar and P. Fayet, "Phenomenology of the production, decay, and detection of new hadronic states associated with supersymmetry", *Phys. Lett. B* **76** (1978) 575–579, doi:10.1016/0370-2693(78)90858-4.

[23] P. Fayet, "Supersymmetric theories of particles and interactions", *Phys. Rept.* **105** (1984) 21, doi:10.1016/0370-1573(84)90113-3.

[24] G. R. Farrar, "Light Gluinos", *Phys. Rev. Lett.* **53** (1984) 1029, doi:10.1103/PhysRevLett.53.1029.

[25] H. Baer, K. Cheung, and J. F. Gunion, "A Heavy gluino as the lightest supersymmetric particle", *Phys. Rev. D* **59** (1999) 075002, doi:10.1103/PhysRevD.59.075002, arXiv:hep-ph/9806361.

[26] A. Mafi and S. Raby, "Analysis of a heavy gluino LSP at CDF: The heavy gluino window", *Phys. Rev. D* **62** (2000) 035003, doi:10.1103/PhysRevD.62.035003, arXiv:hep-ph/9912436.

[27] A. C. Kraan, "Interactions of heavy stable hadronizing particles", *Eur. Phys. J. C* **37** (2004) 91–104, doi:10.1140/epjc/s2004-01997-7, arXiv:hep-ex/0404001.

[28] R. Mackeprang and D. Milstead, "An updated description of heavy-hadron interactions in GEANT4", *Eur. Phys. J C* **66** (2010) 493–501, doi:10.1140/epjc/s10052-010-1262-1, arXiv:0908.1868.

[29] CMS Collaboration, "The CMS experiment at the CERN LHC", *JINST* **03** (2008) S08004, doi:10.1088/1748-0221/3/08/S08004.

[30] S. P. Martin, "A Supersymmetry primer", (1997). arXiv:hep-ph/9709356.

[31] G. L. Kane, ed., "Perspectives on supersymmetry II". World Scientific, 2010. Advanced Series on Directions in High Energy Physics, Vol. 21.

[32] C. Kilic, T. Okui, and R. Sundrum, "Vectorlike confinement at the LHC", *JHEP* **02** (2010) 018, doi:10.1007/JHEP02(2010)018, arXiv:0906.0577.

[33] P. Z. Skands, "Tuning Monte Carlo Generators: The Perugia Tunes", *Phys. Rev. D* **82** (2010) 074018, doi:10.1103/PhysRevD.82.074018, arXiv:1005.3457.

[34] CTEQ Collaboration, "Global QCD analysis of parton structure of the nucleon: CTEQ5 parton distributions", *Eur. Phys. J. C* **12** (2000) 375–392, doi:10.1007/s100529900196, arXiv:hep-ph/9903282.

[35] J. Pumplin et al., "New generation of parton distributions with uncertainties from global QCD analysis", *JHEP* **07** (2002) 012, doi:10.1088/1126-6708/2002/07/012, arXiv:hep-ph/0201195.

[36] T. Sjöstrand, S. Mrenna, and P. Z. Skands, "PYTHIA 6.4 physics and manual", *JHEP* **05** (2006) 026, doi:10.1088/1126-6708/2006/05/026, arXiv:hep-ph/0603175.

[37] N. Arkani-Hamed and S. Dimopoulos, "Supersymmetric unification without low energy supersymmetry and signatures for fine-tuning at the LHC", *JHEP* **06** (2005) 073, doi:10.1088/1126-6708/2005/06/073, arXiv:hep-th/0405159.

[38] G. Giudice and A. Romanino, "Split supersymmetry", *Nucl. Phys. B* **699** (2004) 65–89, doi:10.1016/j.nuclphysb.2004.11.048, arXiv:hep-ph/0406088.

[39] S. Agostinelli et al., "GEANT4–a simulation toolkit", *Nucl. Instrum. Meth. A* **506** (2003) 250, doi:10.1016/S0168-9002(03)01368-8.

[40] J. Allison et al., "Geant4 developments and applications", *IEEE Trans. Nucl. Sci.* **53** (2006) 270 – 278, doi:10.1109/TNS.2006.869826.

[41] R. Mackeprang and A. Rizzi, "Interactions of coloured heavy stable particles in matter", *Eur. Phys. J. C* **50** (2007) 353–362, doi:10.1140/epjc/s10052-007-0252-4, arXiv:hep-ph/0612161.

[42] G. Giudice and R. Rattazzi, "Theories with gauge mediated supersymmetry breaking", *Phys. Rept.* **322** (1999) 419–499, doi:10.1016/S0370-1573(99)00042-3, arXiv:hep-ph/9801271.

[43] B. Allanach et al., "The Snowmass points and slopes: Benchmarks for SUSY searches", *Eur. Phys. J. C* **25** (2002) 113–123, doi:10.1007/s10052-002-0949-3, arXiv:hep-ph/0202233.

[44] F. E. Paige et al., "ISAJET 7.69: A Monte Carlo event generator for pp, anti-p p, and e+e- reactions", arXiv:hep-ph/0312045.

[45] C. Kilic and T. Okui, "The LHC phenomenology of vectorlike confinement", *JHEP* **04** (2010) 128, doi:10.1007/JHEP04(2010)128, arXiv:1001.4526.

[46] J. Chen and T. Adams, "Searching for high speed long-lived charged massive particles at the LHC", *Eur. Phys. J. C* **67** (2010) 335–342, doi:10.1140/epjc/s10052-010-1283-9, arXiv:0909.3157.

[47] A. Pukhov, "CalcHEP 2.3: MSSM, structure functions, event generation, batchs, and generation of matrix elements for other packages", (2004). arXiv:hep-ph/0412191.

[48] CMS Tracker Collaboration, "Performance studies of the CMS Strip Tracker before installation", *JINST* **04** (2009) P06009, doi:10.1088/1748-0221/4/06/P06009, arXiv:0901.4316.

[49] W. T. Eadie et al., "Statistical Methods in Experimental Physics". North Holland, Amsterdam, 1971.

[50] F. James, "Statistical Methods in Experimental Physics". World Scientific, Singapore, 2006.

[51] CMS Collaboration, "CMS tracking performance results from early LHC operation", *Eur. Phys. J. C* **70** (2010) 1165–1192, doi:10.1140/epjc/s10052-010-1491-3, arXiv:1007.1988.

[52] Particle Data Group Collaboration, "Review of particle physics", *J. Phys. G* **37** (2010) 075021, doi:10.1088/0954-3899/37/7A/075021.

[53] CMS Collaboration, "Jet Performance in pp Collisions at $\sqrt{s}$=7 TeV", CMS Physics Analysis Summary CMS-PAS-JME-10-003, (2010).

[54] M. Cacciari, G. P. Salam, and G. Soyez, "The anti-k_t jet clustering algorithm", *JHEP* **04** (2008) 063, doi:10.1088/1126-6708/2008/04/063, arXiv:0802.1189.

[55] A. L. Read, "Modified frequentist analysis of search results (the CL(s) method)", in *Workshop on Confidence Limits*, p. 81. Geneva, Switzerland, 2000.

[56] CMS Collaboration, "Combined results of searches for a standard model Higgs boson", *Phys. Lett. B* **710** (2012) 26, doi:10.1016/j.physletb.2012.02.064, arXiv:1202.1488.

[57] CMS Collaboration, "Determination of Jet Energy Calibration and Transverse Momentum Resolution in CMS", *JINST* **06** (2011) P11002, doi:10.1088/1748-0221/6/11/P11002, arXiv:1107.4277.

[58] CMS Collaboration, "Performance of muon identification in pp collisions at $\sqrt{s}$ = 7 TeV", CMS Physics Analysis Summary CMS-PAS-MUO-10-002, (2010).

[59] CMS Collaboration, "Performance of muon reconstruction in pp collisions at $\sqrt{s}$ = 7 TeV", CMS Physics Analysis Summary CMS-PAS-MUO-10-004, (2012). In preparation—to be released by publication date.

[60] CMS Collaboration, "Measurement of Tracking Efficiency", CMS Physics Analysis Summary CMS-PAS-TRK-10-002, (2010).

[61] CMS Collaboration, "Absolute Calibration of the Luminosity Measurement at CMS: Winter 2012 Update", CMS Physics Analysis Summary CMS-PAS-SMP-12-008, (2012).

[62] A. Kulesza and L. Motyka, "Threshold resummation for squark-antisquark and gluino-pair production at the LHC", *Phys. Rev. Lett.* **102** (2009) 111802, doi:10.1103/PhysRevLett.102.111802, arXiv:0807.2405.

[63] A. Kulesza and L. Motyka, "Soft gluon resummation for the production of gluino-gluino and squark-antisquark pairs at the LHC", *Phys. Rev. D* **80** (2009) 095004, doi:10.1103/PhysRevD.80.095004, arXiv:0905.4749.

[64] W. Beenakker et al., "Soft-gluon resummation for squark and gluino hadroproduction", *JHEP* **12** (2009) 041, doi:10.1088/1126-6708/2009/12/041, arXiv:0909.4418.

[65] W. Beenakker et al., "Supersymmetric top and bottom squark production at hadron colliders", *JHEP* **08** (2010) 098, doi:10.1007/JHEP08(2010)098, arXiv:1006.4771.

[66] W. Beenakker et al., "Squark and gluino hadroproduction", *Int. J. Mod. Phys. A* **26** (2011) 2637–2664, doi:10.1142/S0217751X11053560, arXiv:1105.1110.

[67] W. Beenakker, R. Hopker, and M. Spira, "PROSPINO: A program for the PROduction of Supersymmetric Particles In Next-to-leading Order QCD", (1996). arXiv:hep-ph/9611232.

A The CMS Collaboration

Yerevan Physics Institute, Yerevan, Armenia
S. Chatrchyan, V. Khachatryan, A.M. Sirunyan, A. Tumasyan

Institut für Hochenergiephysik der OeAW, Wien, Austria
W. Adam, T. Bergauer, M. Dragicevic, J. Erö, C. Fabjan, M. Friedl, R. Frühwirth, V.M. Ghete, J. Hammer[1], N. Hörmann, J. Hrubec, M. Jeitler, W. Kiesenhofer, V. Knünz, M. Krammer, D. Liko, I. Mikulec, M. Pernicka[†], B. Rahbaran, C. Rohringer, H. Rohringer, R. Schöfbeck, J. Strauss, A. Taurok, F. Teischinger, P. Wagner, W. Waltenberger, G. Walzel, E. Widl, C.-E. Wulz

National Centre for Particle and High Energy Physics, Minsk, Belarus
V. Mossolov, N. Shumeiko, J. Suarez Gonzalez

Universiteit Antwerpen, Antwerpen, Belgium
S. Bansal, K. Cerny, T. Cornelis, E.A. De Wolf, X. Janssen, S. Luyckx, T. Maes, L. Mucibello, S. Ochesanu, B. Roland, R. Rougny, M. Selvaggi, H. Van Haevermaet, P. Van Mechelen, N. Van Remortel, A. Van Spilbeeck

Vrije Universiteit Brussel, Brussel, Belgium
F. Blekman, S. Blyweert, J. D'Hondt, R. Gonzalez Suarez, A. Kalogeropoulos, M. Maes, A. Olbrechts, W. Van Doninck, P. Van Mulders, G.P. Van Onsem, I. Villella

Université Libre de Bruxelles, Bruxelles, Belgium
O. Charaf, B. Clerbaux, G. De Lentdecker, V. Dero, A.P.R. Gay, T. Hreus, A. Léonard, P.E. Marage, T. Reis, L. Thomas, C. Vander Velde, P. Vanlaer

Ghent University, Ghent, Belgium
V. Adler, K. Beernaert, A. Cimmino, S. Costantini, G. Garcia, M. Grunewald, B. Klein, J. Lellouch, A. Marinov, J. Mccartin, A.A. Ocampo Rios, D. Ryckbosch, N. Strobbe, F. Thyssen, M. Tytgat, L. Vanelderen, P. Verwilligen, S. Walsh, E. Yazgan, N. Zaganidis

Université Catholique de Louvain, Louvain-la-Neuve, Belgium
S. Basegmez, G. Bruno, L. Ceard, C. Delaere, T. du Pree, D. Favart, L. Forthomme, A. Giammanco[2], J. Hollar, V. Lemaitre, J. Liao, O. Militaru, C. Nuttens, D. Pagano, A. Pin, K. Piotrzkowski, N. Schul

Université de Mons, Mons, Belgium
N. Beliy, T. Caebergs, E. Daubie, G.H. Hammad

Centro Brasileiro de Pesquisas Fisicas, Rio de Janeiro, Brazil
G.A. Alves, M. Correa Martins Junior, D. De Jesus Damiao, T. Martins, M.E. Pol, M.H.G. Souza

Universidade do Estado do Rio de Janeiro, Rio de Janeiro, Brazil
W.L. Aldá Júnior, W. Carvalho, A. Custódio, E.M. Da Costa, C. De Oliveira Martins, S. Fonseca De Souza, D. Matos Figueiredo, L. Mundim, H. Nogima, V. Oguri, W.L. Prado Da Silva, A. Santoro, S.M. Silva Do Amaral, L. Soares Jorge, A. Sznajder

Instituto de Fisica Teorica, Universidade Estadual Paulista, Sao Paulo, Brazil
T.S. Anjos[3], C.A. Bernardes[3], F.A. Dias[4], T.R. Fernandez Perez Tomei, E. M. Gregores[3], C. Lagana, F. Marinho, P.G. Mercadante[3], S.F. Novaes, Sandra S. Padula

Institute for Nuclear Research and Nuclear Energy, Sofia, Bulgaria
V. Genchev[1], P. Iaydjiev[1], S. Piperov, M. Rodozov, S. Stoykova, G. Sultanov, V. Tcholakov, R. Trayanov, M. Vutova

University of Sofia, Sofia, Bulgaria
A. Dimitrov, R. Hadjiiska, V. Kozhuharov, L. Litov, B. Pavlov, P. Petkov

Institute of High Energy Physics, Beijing, China
J.G. Bian, G.M. Chen, H.S. Chen, C.H. Jiang, D. Liang, S. Liang, X. Meng, J. Tao, J. Wang, J. Wang, X. Wang, Z. Wang, H. Xiao, M. Xu, J. Zang, Z. Zhang

State Key Lab. of Nucl. Phys. and Tech., Peking University, Beijing, China
C. Asawatangtrakuldee, Y. Ban, S. Guo, Y. Guo, W. Li, S. Liu, Y. Mao, S.J. Qian, H. Teng, S. Wang, B. Zhu, W. Zou

Universidad de Los Andes, Bogota, Colombia
C. Avila, B. Gomez Moreno, A.F. Osorio Oliveros, J.C. Sanabria

Technical University of Split, Split, Croatia
N. Godinovic, D. Lelas, R. Plestina[5], D. Polic, I. Puljak[1]

University of Split, Split, Croatia
Z. Antunovic, M. Dzelalija, M. Kovac

Institute Rudjer Boskovic, Zagreb, Croatia
V. Brigljevic, S. Duric, K. Kadija, J. Luetic, S. Morovic

University of Cyprus, Nicosia, Cyprus
A. Attikis, M. Galanti, G. Mavromanolakis, J. Mousa, C. Nicolaou, F. Ptochos, P.A. Razis

Charles University, Prague, Czech Republic
M. Finger, M. Finger Jr.

Academy of Scientific Research and Technology of the Arab Republic of Egypt, Egyptian Network of High Energy Physics, Cairo, Egypt
Y. Assran[6], S. Elgammal, A. Ellithi Kamel[7], S. Khalil[8], M.A. Mahmoud[9], A. Radi[8,10]

National Institute of Chemical Physics and Biophysics, Tallinn, Estonia
M. Kadastik, M. Müntel, M. Raidal, L. Rebane, A. Tiko

Department of Physics, University of Helsinki, Helsinki, Finland
V. Azzolini, P. Eerola, G. Fedi, M. Voutilainen

Helsinki Institute of Physics, Helsinki, Finland
J. Härkönen, A. Heikkinen, V. Karimäki, R. Kinnunen, M.J. Kortelainen, T. Lampén, K. Lassila-Perini, S. Lehti, T. Lindén, P. Luukka, T. Mäenpää, T. Peltola, E. Tuominen, J. Tuominiemi, E. Tuovinen, D. Ungaro, L. Wendland

Lappeenranta University of Technology, Lappeenranta, Finland
K. Banzuzi, A. Korpela, T. Tuuva

DSM/IRFU, CEA/Saclay, Gif-sur-Yvette, France
M. Besancon, S. Choudhury, M. Dejardin, D. Denegri, B. Fabbro, J.L. Faure, F. Ferri, S. Ganjour, A. Givernaud, P. Gras, G. Hamel de Monchenault, P. Jarry, E. Locci, J. Malcles, L. Millischer, A. Nayak, J. Rander, A. Rosowsky, I. Shreyber, M. Titov

Laboratoire Leprince-Ringuet, Ecole Polytechnique, IN2P3-CNRS, Palaiseau, France
S. Baffioni, F. Beaudette, L. Benhabib, L. Bianchini, M. Bluj[11], C. Broutin, P. Busson, C. Charlot, N. Daci, T. Dahms, L. Dobrzynski, R. Granier de Cassagnac, M. Haguenauer, P. Miné, C. Mironov, C. Ochando, P. Paganini, D. Sabes, R. Salerno, Y. Sirois, C. Veelken, A. Zabi

Institut Pluridisciplinaire Hubert Curien, Université de Strasbourg, Université de Haute Alsace Mulhouse, CNRS/IN2P3, Strasbourg, France
J.-L. Agram[12], J. Andrea, D. Bloch, D. Bodin, J.-M. Brom, M. Cardaci, E.C. Chabert, C. Collard, E. Conte[12], F. Drouhin[12], C. Ferro, J.-C. Fontaine[12], D. Gelé, U. Goerlach, P. Juillot, M. Karim[12], A.-C. Le Bihan, P. Van Hove

Centre de Calcul de l'Institut National de Physique Nucleaire et de Physique des Particules (IN2P3), Villeurbanne, France
F. Fassi, D. Mercier

Université de Lyon, Université Claude Bernard Lyon 1, CNRS-IN2P3, Institut de Physique Nucléaire de Lyon, Villeurbanne, France
S. Beauceron, N. Beaupere, O. Bondu, G. Boudoul, H. Brun, J. Chasserat, R. Chierici[1], D. Contardo, P. Depasse, H. El Mamouni, J. Fay, S. Gascon, M. Gouzevitch, B. Ille, T. Kurca, M. Lethuillier, L. Mirabito, S. Perries, V. Sordini, S. Tosi, Y. Tschudi, P. Verdier, S. Viret

Institute of High Energy Physics and Informatization, Tbilisi State University, Tbilisi, Georgia
Z. Tsamalaidze[13]

RWTH Aachen University, I. Physikalisches Institut, Aachen, Germany
G. Anagnostou, S. Beranek, M. Edelhoff, L. Feld, N. Heracleous, O. Hindrichs, R. Jussen, K. Klein, J. Merz, A. Ostapchuk, A. Perieanu, F. Raupach, J. Sammet, S. Schael, D. Sprenger, H. Weber, B. Wittmer, V. Zhukov[14]

RWTH Aachen University, III. Physikalisches Institut A, Aachen, Germany
M. Ata, J. Caudron, E. Dietz-Laursonn, D. Duchardt, M. Erdmann, A. Güth, T. Hebbeker, C. Heidemann, K. Hoepfner, T. Klimkovich, D. Klingebiel, P. Kreuzer, D. Lanske†, J. Lingemann, C. Magass, M. Merschmeyer, A. Meyer, M. Olschewski, P. Papacz, H. Pieta, H. Reithler, S.A. Schmitz, L. Sonnenschein, J. Steggemann, D. Teyssier, M. Weber

RWTH Aachen University, III. Physikalisches Institut B, Aachen, Germany
M. Bontenackels, V. Cherepanov, M. Davids, G. Flügge, H. Geenen, M. Geisler, W. Haj Ahmad, F. Hoehle, B. Kargoll, T. Kress, Y. Kuessel, A. Linn, A. Nowack, L. Perchalla, O. Pooth, J. Rennefeld, P. Sauerland, A. Stahl

Deutsches Elektronen-Synchrotron, Hamburg, Germany
M. Aldaya Martin, J. Behr, W. Behrenhoff, U. Behrens, M. Bergholz[15], A. Bethani, K. Borras, A. Burgmeier, A. Cakir, L. Calligaris, A. Campbell, E. Castro, F. Costanza, D. Dammann, G. Eckerlin, D. Eckstein, D. Fischer, G. Flucke, A. Geiser, I. Glushkov, S. Habib, J. Hauk, H. Jung[1], M. Kasemann, P. Katsas, C. Kleinwort, H. Kluge, A. Knutsson, M. Krämer, D. Krücker, E. Kuznetsova, W. Lange, W. Lohmann[15], B. Lutz, R. Mankel, I. Marfin, M. Marienfeld, I.-A. Melzer-Pellmann, A.B. Meyer, J. Mnich, A. Mussgiller, S. Naumann-Emme, J. Olzem, H. Perrey, A. Petrukhin, D. Pitzl, A. Raspereza, P.M. Ribeiro Cipriano, C. Riedl, M. Rosin, J. Salfeld-Nebgen, R. Schmidt[15], T. Schoerner-Sadenius, N. Sen, A. Spiridonov, M. Stein, R. Walsh, C. Wissing

University of Hamburg, Hamburg, Germany
C. Autermann, V. Blobel, S. Bobrovskyi, J. Draeger, H. Enderle, J. Erfle, U. Gebbert, M. Görner, T. Hermanns, R.S. Höing, K. Kaschube, G. Kaussen, H. Kirschenmann, R. Klanner, J. Lange, B. Mura, F. Nowak, N. Pietsch, D. Rathjens, C. Sander, H. Schettler, P. Schleper, E. Schlieckau, A. Schmidt, M. Schröder, T. Schum, M. Seidel, H. Stadie, G. Steinbrück, J. Thomsen

Institut für Experimentelle Kernphysik, Karlsruhe, Germany
C. Barth, J. Berger, T. Chwalek, W. De Boer, A. Dierlamm, M. Feindt, M. Guthoff[1], C. Hackstein, F. Hartmann, M. Heinrich, H. Held, K.H. Hoffmann, S. Honc, I. Katkov[14], J.R. Komaragiri, D. Martschei, S. Mueller, Th. Müller, M. Niegel, A. Nürnberg, O. Oberst, A. Oehler, J. Ott, T. Peiffer, G. Quast, K. Rabbertz, F. Ratnikov, N. Ratnikova, S. Röcker, C. Saout, A. Scheurer, F.-P. Schilling, M. Schmanau, G. Schott, H.J. Simonis, F.M. Stober, D. Troendle, R. Ulrich, J. Wagner-Kuhr, T. Weiler, M. Zeise, E.B. Ziebarth

Institute of Nuclear Physics "Demokritos", Aghia Paraskevi, Greece
G. Daskalakis, T. Geralis, S. Kesisoglou, A. Kyriakis, D. Loukas, I. Manolakos, A. Markou, C. Markou, C. Mavrommatis, E. Ntomari

University of Athens, Athens, Greece
L. Gouskos, T.J. Mertzimekis, A. Panagiotou, N. Saoulidou

University of Ioánnina, Ioánnina, Greece
I. Evangelou, C. Foudas[1], P. Kokkas, N. Manthos, I. Papadopoulos, V. Patras

KFKI Research Institute for Particle and Nuclear Physics, Budapest, Hungary
G. Bencze, C. Hajdu[1], P. Hidas, D. Horvath[16], K. Krajczar[17], B. Radics, F. Sikler[1], V. Veszpremi, G. Vesztergombi[17]

Institute of Nuclear Research ATOMKI, Debrecen, Hungary
N. Beni, S. Czellar, J. Molnar, J. Palinkas, Z. Szillasi

University of Debrecen, Debrecen, Hungary
J. Karancsi, P. Raics, Z.L. Trocsanyi, B. Ujvari

Panjab University, Chandigarh, India
S.B. Beri, V. Bhatnagar, N. Dhingra, R. Gupta, M. Jindal, M. Kaur, J.M. Kohli, M.Z. Mehta, N. Nishu, L.K. Saini, A. Sharma, J. Singh, S.P. Singh

University of Delhi, Delhi, India
S. Ahuja, A. Bhardwaj, B.C. Choudhary, A. Kumar, A. Kumar, S. Malhotra, M. Naimuddin, K. Ranjan, V. Sharma, R.K. Shivpuri

Saha Institute of Nuclear Physics, Kolkata, India
S. Banerjee, S. Bhattacharya, S. Dutta, B. Gomber, Sa. Jain, Sh. Jain, R. Khurana, S. Sarkar

Bhabha Atomic Research Centre, Mumbai, India
A. Abdulsalam, R.K. Choudhury, D. Dutta, S. Kailas, V. Kumar, A.K. Mohanty[1], L.M. Pant, P. Shukla

Tata Institute of Fundamental Research - EHEP, Mumbai, India
T. Aziz, S. Ganguly, M. Guchait[18], A. Gurtu[19], M. Maity[20], G. Majumder, K. Mazumdar, G.B. Mohanty, B. Parida, K. Sudhakar, N. Wickramage

Tata Institute of Fundamental Research - HECR, Mumbai, India
S. Banerjee, S. Dugad

Institute for Research in Fundamental Sciences (IPM), Tehran, Iran
H. Arfaei, H. Bakhshiansohi[21], S.M. Etesami[22], A. Fahim[21], M. Hashemi, H. Hesari, A. Jafari[21], M. Khakzad, A. Mohammadi[23], M. Mohammadi Najafabadi, S. Paktinat Mehdiabadi, B. Safarzadeh[24], M. Zeinali[22]

INFN Sezione di Bari [a], Università di Bari [b], Politecnico di Bari [c], Bari, Italy
M. Abbrescia[a,b], L. Barbone[a,b], C. Calabria[a,b,1], S.S. Chhibra[a,b], A. Colaleo[a], D. Creanza[a,c], N. De Filippis[a,c,1], M. De Palma[a,b], L. Fiore[a], G. Iaselli[a,c], L. Lusito[a,b], G. Maggi[a,c], M. Maggi[a], B. Marangelli[a,b], S. My[a,c], S. Nuzzo[a,b], N. Pacifico[a,b], A. Pompili[a,b], G. Pugliese[a,c], G. Selvaggi[a,b], L. Silvestris[a], G. Singh[a,b], G. Zito[a]

INFN Sezione di Bologna [a], Università di Bologna [b], Bologna, Italy
G. Abbiendi[a], A.C. Benvenuti[a], D. Bonacorsi[a,b], S. Braibant-Giacomelli[a,b], L. Brigliadori[a,b], P. Capiluppi[a,b], A. Castro[a,b], F.R. Cavallo[a], M. Cuffiani[a,b], G.M. Dallavalle[a], F. Fabbri[a], A. Fanfani[a,b], D. Fasanella[a,b,1], P. Giacomelli[a], C. Grandi[a], L. Guiducci, S. Marcellini[a], G. Masetti[a], M. Meneghelli[a,b,1], A. Montanari[a], F.L. Navarria[a,b], F. Odorici[a], A. Perrotta[a], F. Primavera[a,b], A.M. Rossi[a,b], T. Rovelli[a,b], G. Siroli[a,b], R. Travaglini[a,b]

INFN Sezione di Catania [a], Università di Catania [b], Catania, Italy
S. Albergo[a,b], G. Cappello[a,b], M. Chiorboli[a,b], S. Costa[a,b], R. Potenza[a,b], A. Tricomi[a,b], C. Tuve[a,b]

INFN Sezione di Firenze [a], Università di Firenze [b], Firenze, Italy
G. Barbagli[a], V. Ciulli[a,b], C. Civinini[a], R. D'Alessandro[a,b], E. Focardi[a,b], S. Frosali[a,b], E. Gallo[a], S. Gonzi[a,b], M. Meschini[a], S. Paoletti[a], G. Sguazzoni[a], A. Tropiano[a,1]

INFN Laboratori Nazionali di Frascati, Frascati, Italy
L. Benussi, S. Bianco, S. Colafranceschi[25], F. Fabbri, D. Piccolo

INFN Sezione di Genova, Genova, Italy
P. Fabbricatore, R. Musenich

INFN Sezione di Milano-Bicocca [a], Università di Milano-Bicocca [b], Milano, Italy
A. Benaglia[a,b,1], F. De Guio[a,b], L. Di Matteo[a,b,1], S. Fiorendi[a,b], S. Gennai[a,1], A. Ghezzi[a,b], S. Malvezzi[a], R.A. Manzoni[a,b], A. Martelli[a,b], A. Massironi[a,b,1], D. Menasce[a], L. Moroni[a], M. Paganoni[a,b], D. Pedrini[a], S. Ragazzi[a,b], N. Redaelli[a], S. Sala[a], T. Tabarelli de Fatis[a,b]

INFN Sezione di Napoli [a], Università di Napoli "Federico II" [b], Napoli, Italy
S. Buontempo[a], C.A. Carrillo Montoya[a,1], N. Cavallo[a,26], A. De Cosa[a,b], O. Dogangun[a,b], F. Fabozzi[a,26], A.O.M. Iorio[a,1], L. Lista[a], S. Meola[a,27], M. Merola[a,b], P. Paolucci[a]

INFN Sezione di Padova [a], Università di Padova [b], Università di Trento (Trento) [c], Padova, Italy
P. Azzi[a], N. Bacchetta[a,1], P. Bellan[a,b], D. Bisello[a,b], A. Branca[a,1], R. Carlin[a,b], P. Checchia[a], T. Dorigo[a], F. Gasparini[a,b], U. Gasparini[a,b], A. Gozzelino[a], K. Kanishchev[a,c], S. Lacaprara[a], I. Lazzizzera[a,c], M. Margoni[a,b], A.T. Meneguzzo[a,b], M. Nespolo[a,1], L. Perrozzi[a], N. Pozzobon[a,b], P. Ronchese[a,b], F. Simonetto[a,b], E. Torassa[a], M. Tosi[a,b,1], S. Vanini[a,b], P. Zotto[a,b]

INFN Sezione di Pavia [a], Università di Pavia [b], Pavia, Italy
M. Gabusi[a,b], S.P. Ratti[a,b], C. Riccardi[a,b], P. Torre[a,b], P. Vitulo[a,b]

INFN Sezione di Perugia [a], Università di Perugia [b], Perugia, Italy
G.M. Bilei[a], L. Fanò[a,b], P. Lariccia[a,b], A. Lucaroni[a,b,1], G. Mantovani[a,b], M. Menichelli[a], A. Nappi[a,b], F. Romeo[a,b], A. Saha, A. Santocchia[a,b], S. Taroni[a,b,1]

INFN Sezione di Pisa [a], Università di Pisa [b], Scuola Normale Superiore di Pisa [c], Pisa, Italy
P. Azzurri[a,c], G. Bagliesi[a], T. Boccali[a], G. Broccolo[a,c], R. Castaldi[a], R.T. D'Agnolo[a,c], R. Dell'Orso[a], F. Fiori[a,b,1], L. Foà[a,c], A. Giassi[a], A. Kraan[a], F. Ligabue[a,c], T. Lomtadze[a], L. Martini[a,28], A. Messineo[a,b], F. Palla[a], F. Palmonari[a], A. Rizzi[a,b], A.T. Serban[a,29], P. Spagnolo[a], P. Squillacioti[1], R. Tenchini[a], G. Tonelli[a,b,1], A. Venturi[a,1], P.G. Verdini[a]

INFN Sezione di Roma [a], Università di Roma "La Sapienza" [b], Roma, Italy
L. Barone[a,b], F. Cavallari[a], D. Del Re[a,b,1], M. Diemoz[a], C. Fanelli[a,b], M. Grassi[a,1], E. Longo[a,b], P. Meridiani[a,1], F. Micheli[a,b], S. Nourbakhsh[a], G. Organtini[a,b], F. Pandolfi[a,b], R. Paramatti[a], S. Rahatlou[a,b], M. Sigamani[a], L. Soffi[a,b]

INFN Sezione di Torino [a], Università di Torino [b], Università del Piemonte Orientale (Novara) [c], Torino, Italy
N. Amapane[a,b], R. Arcidiacono[a,c], S. Argiro[a,b], M. Arneodo[a,c], C. Biino[a], C. Botta[a,b], N. Cartiglia[a], R. Castello[a,b], M. Costa[a,b], G. Dellacasa[a], N. Demaria[a], A. Graziano[a,b], C. Mariotti[a,1], S. Maselli[a], E. Migliore[a,b], V. Monaco[a,b], M. Musich[a,1], M.M. Obertino[a,c], N. Pastrone[a], M. Pelliccioni[a], A. Potenza[a,b], A. Romero[a,b], M. Ruspa[a,c], R. Sacchi[a,b], A. Solano[a,b], A. Staiano[a], A. Vilela Pereira[a]

INFN Sezione di Trieste [a], Università di Trieste [b], Trieste, Italy
S. Belforte[a], F. Cossutti[a], G. Della Ricca[a,b], B. Gobbo[a], M. Marone[a,b,1], D. Montanino[a,b,1], A. Penzo[a], A. Schizzi[a,b]

Kangwon National University, Chunchon, Korea
S.G. Heo, T.Y. Kim, S.K. Nam

Kyungpook National University, Daegu, Korea
S. Chang, J. Chung, D.H. Kim, G.N. Kim, D.J. Kong, H. Park, S.R. Ro, D.C. Son, T. Son

Chonnam National University, Institute for Universe and Elementary Particles, Kwangju, Korea
J.Y. Kim, Zero J. Kim, S. Song

Konkuk University, Seoul, Korea
H.Y. Jo

Korea University, Seoul, Korea
S. Choi, D. Gyun, B. Hong, M. Jo, H. Kim, T.J. Kim, K.S. Lee, D.H. Moon, S.K. Park, E. Seo

University of Seoul, Seoul, Korea
M. Choi, S. Kang, H. Kim, J.H. Kim, C. Park, I.C. Park, S. Park, G. Ryu

Sungkyunkwan University, Suwon, Korea
Y. Cho, Y. Choi, Y.K. Choi, J. Goh, M.S. Kim, E. Kwon, B. Lee, J. Lee, S. Lee, H. Seo, I. Yu

Vilnius University, Vilnius, Lithuania
M.J. Bilinskas, I. Grigelionis, M. Janulis, A. Juodagalvis

Centro de Investigacion y de Estudios Avanzados del IPN, Mexico City, Mexico
H. Castilla-Valdez, E. De La Cruz-Burelo, I. Heredia-de La Cruz, R. Lopez-Fernandez, R. Magaña Villalba, J. Martínez-Ortega, A. Sánchez-Hernández, L.M. Villasenor-Cendejas

Universidad Iberoamericana, Mexico City, Mexico
S. Carrillo Moreno, F. Vazquez Valencia

Benemerita Universidad Autonoma de Puebla, Puebla, Mexico
H.A. Salazar Ibarguen

Universidad Autónoma de San Luis Potosí, San Luis Potosí, Mexico
E. Casimiro Linares, A. Morelos Pineda, M.A. Reyes-Santos

University of Auckland, Auckland, New Zealand
D. Krofcheck

University of Canterbury, Christchurch, New Zealand
A.J. Bell, P.H. Butler, R. Doesburg, S. Reucroft, H. Silverwood

National Centre for Physics, Quaid-I-Azam University, Islamabad, Pakistan
M. Ahmad, M.I. Asghar, H.R. Hoorani, S. Khalid, W.A. Khan, T. Khurshid, S. Qazi, M.A. Shah, M. Shoaib

Institute of Experimental Physics, Faculty of Physics, University of Warsaw, Warsaw, Poland
G. Brona, K. Bunkowski, M. Cwiok, W. Dominik, K. Doroba, A. Kalinowski, M. Konecki, J. Krolikowski

Soltan Institute for Nuclear Studies, Warsaw, Poland
H. Bialkowska, B. Boimska, T. Frueboes, R. Gokieli, M. Górski, M. Kazana, K. Nawrocki, K. Romanowska-Rybinska, M. Szleper, G. Wrochna, P. Zalewski

Laboratório de Instrumentação e Física Experimental de Partículas, Lisboa, Portugal
N. Almeida, P. Bargassa, A. David, P. Faccioli, P.G. Ferreira Parracho, M. Gallinaro, P. Musella, J. Seixas, J. Varela, P. Vischia

Joint Institute for Nuclear Research, Dubna, Russia
I. Belotelov, P. Bunin, M. Gavrilenko, I. Golutvin, A. Kamenev, V. Karjavin, G. Kozlov, A. Lanev, A. Malakhov, P. Moisenz, V. Palichik, V. Perelygin, M. Savina, S. Shmatov, V. Smirnov, A. Volodko, A. Zarubin

Petersburg Nuclear Physics Institute, Gatchina (St Petersburg), Russia
S. Evstyukhin, V. Golovtsov, Y. Ivanov, V. Kim, P. Levchenko, V. Murzin, V. Oreshkin, I. Smirnov, V. Sulimov, L. Uvarov, S. Vavilov, A. Vorobyev, An. Vorobyev

Institute for Nuclear Research, Moscow, Russia
Yu. Andreev, A. Dermenev, S. Gninenko, N. Golubev, M. Kirsanov, N. Krasnikov, V. Matveev, A. Pashenkov, D. Tlisov, A. Toropin

Institute for Theoretical and Experimental Physics, Moscow, Russia
V. Epshteyn, M. Erofeeva, V. Gavrilov, M. Kossov[1], N. Lychkovskaya, V. Popov, G. Safronov, S. Semenov, V. Stolin, E. Vlasov, A. Zhokin

Moscow State University, Moscow, Russia
A. Belyaev, E. Boos, M. Dubinin[4], L. Dudko, A. Ershov, A. Gribushin, V. Klyukhin, O. Kodolova, I. Lokhtin, A. Markina, S. Obraztsov, M. Perfilov, S. Petrushanko, A. Popov, L. Sarycheva†, V. Savrin, A. Snigirev

P.N. Lebedev Physical Institute, Moscow, Russia
V. Andreev, M. Azarkin, I. Dremin, M. Kirakosyan, A. Leonidov, G. Mesyats, S.V. Rusakov, A. Vinogradov

State Research Center of Russian Federation, Institute for High Energy Physics, Protvino, Russia
I. Azhgirey, I. Bayshev, S. Bitioukov, V. Grishin[1], V. Kachanov, D. Konstantinov, A. Korablev, V. Krychkine, V. Petrov, R. Ryutin, A. Sobol, L. Tourtchanovitch, S. Troshin, N. Tyurin, A. Uzunian, A. Volkov

University of Belgrade, Faculty of Physics and Vinca Institute of Nuclear Sciences, Belgrade, Serbia
P. Adzic[30], M. Djordjevic, M. Ekmedzic, D. Krpic[30], J. Milosevic

Centro de Investigaciones Energéticas Medioambientales y Tecnológicas (CIEMAT), Madrid, Spain
M. Aguilar-Benitez, J. Alcaraz Maestre, P. Arce, C. Battilana, E. Calvo, M. Cerrada, M. Chamizo Llatas, N. Colino, B. De La Cruz, A. Delgado Peris, C. Diez Pardos, D. Domínguez Vázquez, C. Fernandez Bedoya, J.P. Fernández Ramos, A. Ferrando, J. Flix, M.C. Fouz, P. Garcia-Abia, O. Gonzalez Lopez, S. Goy Lopez, J.M. Hernandez, M.I. Josa, G. Merino, J. Puerta Pelayo, I. Redondo, L. Romero, J. Santaolalla, M.S. Soares, C. Willmott

Universidad Autónoma de Madrid, Madrid, Spain
C. Albajar, G. Codispoti, J.F. de Trocóniz

Universidad de Oviedo, Oviedo, Spain
J. Cuevas, J. Fernandez Menendez, S. Folgueras, I. Gonzalez Caballero, L. Lloret Iglesias, J. Piedra Gomez[31], J.M. Vizan Garcia

Instituto de Física de Cantabria (IFCA), CSIC-Universidad de Cantabria, Santander, Spain
J.A. Brochero Cifuentes, I.J. Cabrillo, A. Calderon, S.H. Chuang, J. Duarte Campderros, M. Felcini[32], M. Fernandez, G. Gomez, J. Gonzalez Sanchez, C. Jorda, P. Lobelle Pardo, A. Lopez Virto, J. Marco, R. Marco, C. Martinez Rivero, F. Matorras, F.J. Munoz Sanchez, T. Rodrigo, A.Y. Rodríguez-Marrero, A. Ruiz-Jimeno, L. Scodellaro, M. Sobron Sanudo, I. Vila, R. Vilar Cortabitarte

CERN, European Organization for Nuclear Research, Geneva, Switzerland
D. Abbaneo, E. Auffray, G. Auzinger, P. Baillon, A.H. Ball, D. Barney, C. Bernet[5], G. Bianchi, P. Bloch, A. Bocci, A. Bonato, H. Breuker, T. Camporesi, G. Cerminara, T. Christiansen, J.A. Coarasa Perez, D. D'Enterria, A. De Roeck, S. Di Guida, M. Dobson, N. Dupont-Sagorin, A. Elliott-Peisert, B. Frisch, W. Funk, G. Georgiou, M. Giffels, D. Gigi, K. Gill, D. Giordano, M. Giunta, F. Glege, R. Gomez-Reino Garrido, P. Govoni, S. Gowdy, R. Guida, M. Hansen, P. Harris, C. Hartl, J. Harvey, B. Hegner, A. Hinzmann, V. Innocente, P. Janot, K. Kaadze, E. Karavakis, K. Kousouris, P. Lecoq, P. Lenzi, C. Lourenço, T. Mäki, M. Malberti, L. Malgeri, M. Mannelli, L. Masetti, F. Meijers, S. Mersi, E. Meschi, R. Moser, M.U. Mozer, M. Mulders, E. Nesvold, M. Nguyen, T. Orimoto, L. Orsini, E. Palencia Cortezon, E. Perez, A. Petrilli, A. Pfeiffer, M. Pierini, M. Pimiä, D. Piparo, G. Polese, L. Quertenmont, A. Racz, W. Reece, J. Rodrigues Antunes, G. Rolandi[33], T. Rommerskirchen, C. Rovelli[34], M. Rovere, H. Sakulin, F. Santanastasio, C. Schäfer, C. Schwick, I. Segoni, S. Sekmen, A. Sharma, P. Siegrist, P. Silva, M. Simon, P. Sphicas[35], D. Spiga, M. Spiropulu[4], M. Stoye, A. Tsirou, G.I. Veres[17], J.R. Vlimant, H.K. Wöhri, S.D. Worm[36], W.D. Zeuner

Paul Scherrer Institut, Villigen, Switzerland
W. Bertl, K. Deiters, W. Erdmann, K. Gabathuler, R. Horisberger, Q. Ingram, H.C. Kaestli, S. König, D. Kotlinski, U. Langenegger, F. Meier, D. Renker, T. Rohe, J. Sibille[37]

Institute for Particle Physics, ETH Zurich, Zurich, Switzerland
L. Bäni, P. Bortignon, M.A. Buchmann, B. Casal, N. Chanon, Z. Chen, A. Deisher, G. Dissertori, M. Dittmar, M. Dünser, J. Eugster, K. Freudenreich, C. Grab, P. Lecomte, W. Lustermann, A.C. Marini, P. Martinez Ruiz del Arbol, N. Mohr, F. Moortgat, C. Nägeli[38], P. Nef, F. Nessi-Tedaldi, L. Pape, F. Pauss, M. Peruzzi, F.J. Ronga, M. Rossini, L. Sala, A.K. Sanchez, A. Starodumov[39], B. Stieger, M. Takahashi, L. Tauscher[†], A. Thea, K. Theofilatos, D. Treille, C. Urscheler, R. Wallny, H.A. Weber, L. Wehrli

Universität Zürich, Zurich, Switzerland
E. Aguilo, C. Amsler, V. Chiochia, S. De Visscher, C. Favaro, M. Ivova Rikova, B. Millan Mejias, P. Otiougova, P. Robmann, H. Snoek, S. Tupputi, M. Verzetti

National Central University, Chung-Li, Taiwan
Y.H. Chang, K.H. Chen, A. Go, C.M. Kuo, S.W. Li, W. Lin, Z.K. Liu, Y.J. Lu, D. Mekterovic, A.P. Singh, R. Volpe, S.S. Yu

National Taiwan University (NTU), Taipei, Taiwan
P. Bartalini, P. Chang, Y.H. Chang, Y.W. Chang, Y. Chao, K.F. Chen, C. Dietz, U. Grundler, W.-S. Hou, Y. Hsiung, K.Y. Kao, Y.J. Lei, R.-S. Lu, D. Majumder, E. Petrakou, X. Shi, J.G. Shiu, Y.M. Tzeng, M. Wang

Cukurova University, Adana, Turkey
A. Adiguzel, M.N. Bakirci[40], S. Cerci[41], C. Dozen, I. Dumanoglu, E. Eskut, S. Girgis, G. Gokbulut, I. Hos, E.E. Kangal, G. Karapinar, A. Kayis Topaksu, G. Onengut, K. Ozdemir, S. Ozturk[42], A. Polatoz, K. Sogut[43], D. Sunar Cerci[41], B. Tali[41], H. Topakli[40], L.N. Vergili, M. Vergili

Middle East Technical University, Physics Department, Ankara, Turkey
I.V. Akin, T. Aliev, B. Bilin, S. Bilmis, M. Deniz, H. Gamsizkan, A.M. Guler, K. Ocalan, A. Ozpineci, M. Serin, R. Sever, U.E. Surat, M. Yalvac, E. Yildirim, M. Zeyrek

Bogazici University, Istanbul, Turkey
M. Deliomeroglu, E. Gülmez, B. Isildak, M. Kaya[44], O. Kaya[44], S. Ozkorucuklu[45], N. Sonmez[46]

Istanbul Technical University, Istanbul, Turkey
K. Cankocak

National Scientific Center, Kharkov Institute of Physics and Technology, Kharkov, Ukraine
L. Levchuk

University of Bristol, Bristol, United Kingdom
F. Bostock, J.J. Brooke, E. Clement, D. Cussans, H. Flacher, R. Frazier, J. Goldstein, M. Grimes, G.P. Heath, H.F. Heath, L. Kreczko, S. Metson, D.M. Newbold[36], K. Nirunpong, A. Poll, S. Senkin, V.J. Smith, T. Williams

Rutherford Appleton Laboratory, Didcot, United Kingdom
L. Basso[47], K.W. Bell, A. Belyaev[47], C. Brew, R.M. Brown, D.J.A. Cockerill, J.A. Coughlan, K. Harder, S. Harper, J. Jackson, B.W. Kennedy, E. Olaiya, D. Petyt, B.C. Radburn-Smith, C.H. Shepherd-Themistocleous, I.R. Tomalin, W.J. Womersley

Imperial College, London, United Kingdom
R. Bainbridge, G. Ball, R. Beuselinck, O. Buchmuller, D. Colling, N. Cripps, M. Cutajar, P. Dauncey, G. Davies, M. Della Negra, W. Ferguson, J. Fulcher, D. Futyan, A. Gilbert, A. Guneratne Bryer, G. Hall, Z. Hatherell, J. Hays, G. Iles, M. Jarvis, G. Karapostoli, L. Lyons, A.-M. Magnan, J. Marrouche, B. Mathias, R. Nandi, J. Nash, A. Nikitenko[39], A. Papageorgiou, J. Pela[1], M. Pesaresi, K. Petridis, M. Pioppi[48], D.M. Raymond, S. Rogerson, N. Rompotis, A. Rose, M.J. Ryan, C. Seez, P. Sharp[†], A. Sparrow, A. Tapper, M. Vazquez Acosta, T. Virdee, S. Wakefield, N. Wardle, T. Whyntie

Brunel University, Uxbridge, United Kingdom
M. Barrett, M. Chadwick, J.E. Cole, P.R. Hobson, A. Khan, P. Kyberd, D. Leggat, D. Leslie, W. Martin, I.D. Reid, P. Symonds, L. Teodorescu, M. Turner

Baylor University, Waco, USA
K. Hatakeyama, H. Liu, T. Scarborough

The University of Alabama, Tuscaloosa, USA
C. Henderson, P. Rumerio

Boston University, Boston, USA
A. Avetisyan, T. Bose, C. Fantasia, A. Heister, J. St. John, P. Lawson, D. Lazic, J. Rohlf, D. Sperka, L. Sulak

Brown University, Providence, USA
J. Alimena, S. Bhattacharya, D. Cutts, A. Ferapontov, U. Heintz, S. Jabeen, G. Kukartsev, G. Landsberg, M. Luk, M. Narain, D. Nguyen, M. Segala, T. Sinthuprasith, T. Speer, K.V. Tsang

University of California, Davis, Davis, USA
R. Breedon, G. Breto, M. Calderon De La Barca Sanchez, S. Chauhan, M. Chertok, J. Conway, R. Conway, P.T. Cox, J. Dolen, R. Erbacher, M. Gardner, R. Houtz, W. Ko, A. Kopecky, R. Lander, O. Mall, T. Miceli, R. Nelson, D. Pellett, B. Rutherford, M. Searle, J. Smith, M. Squires, M. Tripathi, R. Vasquez Sierra

University of California, Los Angeles, Los Angeles, USA
V. Andreev, D. Cline, R. Cousins, J. Duris, S. Erhan, P. Everaerts, C. Farrell, J. Hauser, M. Ignatenko, C. Plager, G. Rakness, P. Schlein†, J. Tucker, V. Valuev, M. Weber

University of California, Riverside, Riverside, USA
J. Babb, R. Clare, M.E. Dinardo, J. Ellison, J.W. Gary, F. Giordano, G. Hanson, G.Y. Jeng[49], H. Liu, O.R. Long, A. Luthra, H. Nguyen, S. Paramesvaran, J. Sturdy, S. Sumowidagdo, R. Wilken, S. Wimpenny

University of California, San Diego, La Jolla, USA
W. Andrews, J.G. Branson, G.B. Cerati, S. Cittolin, D. Evans, F. Golf, A. Holzner, R. Kelley, M. Lebourgeois, J. Letts, I. Macneill, B. Mangano, J. Muelmenstaedt, S. Padhi, C. Palmer, G. Petrucciani, M. Pieri, R. Ranieri, M. Sani, V. Sharma, S. Simon, E. Sudano, M. Tadel, Y. Tu, A. Vartak, S. Wasserbaech[50], F. Würthwein, A. Yagil, J. Yoo

University of California, Santa Barbara, Santa Barbara, USA
D. Barge, R. Bellan, C. Campagnari, M. D'Alfonso, T. Danielson, K. Flowers, P. Geffert, J. Incandela, C. Justus, P. Kalavase, S.A. Koay, D. Kovalskyi[1], V. Krutelyov, S. Lowette, N. Mccoll, V. Pavlunin, F. Rebassoo, J. Ribnik, J. Richman, R. Rossin, D. Stuart, W. To, C. West

California Institute of Technology, Pasadena, USA
A. Apresyan, A. Bornheim, Y. Chen, E. Di Marco, J. Duarte, M. Gataullin, Y. Ma, A. Mott, H.B. Newman, C. Rogan, V. Timciuc, P. Traczyk, J. Veverka, R. Wilkinson, Y. Yang, R.Y. Zhu

Carnegie Mellon University, Pittsburgh, USA
B. Akgun, R. Carroll, T. Ferguson, Y. Iiyama, D.W. Jang, Y.F. Liu, M. Paulini, H. Vogel, I. Vorobiev

University of Colorado at Boulder, Boulder, USA
J.P. Cumalat, B.R. Drell, C.J. Edelmaier, W.T. Ford, A. Gaz, B. Heyburn, E. Luiggi Lopez, J.G. Smith, K. Stenson, K.A. Ulmer, S.R. Wagner

Cornell University, Ithaca, USA
L. Agostino, J. Alexander, A. Chatterjee, N. Eggert, L.K. Gibbons, B. Heltsley, W. Hopkins, A. Khukhunaishvili, B. Kreis, N. Mirman, G. Nicolas Kaufman, J.R. Patterson, A. Ryd, E. Salvati, W. Sun, W.D. Teo, J. Thom, J. Thompson, J. Vaughan, Y. Weng, L. Winstrom, P. Wittich

Fairfield University, Fairfield, USA
D. Winn

Fermi National Accelerator Laboratory, Batavia, USA
S. Abdullin, M. Albrow, J. Anderson, L.A.T. Bauerdick, A. Beretvas, J. Berryhill, P.C. Bhat, I. Bloch, K. Burkett, J.N. Butler, V. Chetluru, H.W.K. Cheung, F. Chlebana, V.D. Elvira, I. Fisk, J. Freeman, Y. Gao, D. Green, O. Gutsche, A. Hahn, J. Hanlon, R.M. Harris, J. Hirschauer, B. Hooberman, S. Jindariani, M. Johnson, U. Joshi, B. Kilminster, B. Klima, S. Kunori, S. Kwan, D. Lincoln, R. Lipton, L. Lueking, J. Lykken, K. Maeshima, J.M. Marraffino, S. Maruyama, D. Mason, P. McBride, K. Mishra, S. Mrenna, Y. Musienko[51], C. Newman-Holmes, V. O'Dell, O. Prokofyev, E. Sexton-Kennedy, S. Sharma, W.J. Spalding, L. Spiegel, P. Tan, L. Taylor, S. Tkaczyk, N.V. Tran, L. Uplegger, E.W. Vaandering, R. Vidal, J. Whitmore, W. Wu, F. Yang, F. Yumiceva, J.C. Yun

University of Florida, Gainesville, USA
D. Acosta, P. Avery, D. Bourilkov, M. Chen, S. Das, M. De Gruttola, G.P. Di Giovanni, D. Dobur, A. Drozdetskiy, R.D. Field, M. Fisher, Y. Fu, I.K. Furic, J. Gartner, J. Hugon, B. Kim, J. Konigsberg, A. Korytov, A. Kropivnitskaya, T. Kypreos, J.F. Low, K. Matchev, P. Milenovic[52], G. Mitselmakher, L. Muniz, R. Remington, A. Rinkevicius, P. Sellers, N. Skhirtladze, M. Snowball, J. Yelton, M. Zakaria

Florida International University, Miami, USA
V. Gaultney, L.M. Lebolo, S. Linn, P. Markowitz, G. Martinez, J.L. Rodriguez

Florida State University, Tallahassee, USA
T. Adams, A. Askew, J. Bochenek, J. Chen, B. Diamond, S.V. Gleyzer, J. Haas, S. Hagopian, V. Hagopian, M. Jenkins, K.F. Johnson, H. Prosper, V. Veeraraghavan, M. Weinberg

Florida Institute of Technology, Melbourne, USA
M.M. Baarmand, B. Dorney, M. Hohlmann, H. Kalakhety, I. Vodopiyanov

University of Illinois at Chicago (UIC), Chicago, USA
M.R. Adams, I.M. Anghel, L. Apanasevich, Y. Bai, V.E. Bazterra, R.R. Betts, J. Callner, R. Cavanaugh, C. Dragoiu, O. Evdokimov, E.J. Garcia-Solis, L. Gauthier, C.E. Gerber, D.J. Hofman, S. Khalatyan, F. Lacroix, M. Malek, C. O'Brien, C. Silkworth, D. Strom, N. Varelas

The University of Iowa, Iowa City, USA
U. Akgun, E.A. Albayrak, B. Bilki[53], K. Chung, W. Clarida, F. Duru, S. Griffiths, C.K. Lae, J.-P. Merlo, H. Mermerkaya[54], A. Mestvirishvili, A. Moeller, J. Nachtman, C.R. Newsom, E. Norbeck, J. Olson, Y. Onel, F. Ozok, S. Sen, E. Tiras, J. Wetzel, T. Yetkin, K. Yi

Johns Hopkins University, Baltimore, USA
B.A. Barnett, B. Blumenfeld, S. Bolognesi, D. Fehling, G. Giurgiu, A.V. Gritsan, Z.J. Guo, G. Hu, P. Maksimovic, S. Rappoccio, M. Swartz, A. Whitbeck

The University of Kansas, Lawrence, USA
P. Baringer, A. Bean, G. Benelli, O. Grachov, R.P. Kenny Iii, M. Murray, D. Noonan, V. Radicci, S. Sanders, R. Stringer, G. Tinti, J.S. Wood, V. Zhukova

Kansas State University, Manhattan, USA
A.F. Barfuss, T. Bolton, I. Chakaberia, A. Ivanov, S. Khalil, M. Makouski, Y. Maravin, S. Shrestha, I. Svintradze

Lawrence Livermore National Laboratory, Livermore, USA
J. Gronberg, D. Lange, D. Wright

University of Maryland, College Park, USA
A. Baden, M. Boutemeur, B. Calvert, S.C. Eno, J.A. Gomez, N.J. Hadley, R.G. Kellogg, M. Kirn, T. Kolberg, Y. Lu, M. Marionneau, A.C. Mignerey, A. Peterman, K. Rossato, A. Skuja, J. Temple, M.B. Tonjes, S.C. Tonwar, E. Twedt

Massachusetts Institute of Technology, Cambridge, USA
G. Bauer, J. Bendavid, W. Busza, E. Butz, I.A. Cali, M. Chan, V. Dutta, G. Gomez Ceballos, M. Goncharov, K.A. Hahn, Y. Kim, M. Klute, Y.-J. Lee, W. Li, P.D. Luckey, T. Ma, S. Nahn, C. Paus, D. Ralph, C. Roland, G. Roland, M. Rudolph, G.S.F. Stephans, F. Stöckli, K. Sumorok, K. Sung, D. Velicanu, E.A. Wenger, R. Wolf, B. Wyslouch, S. Xie, M. Yang, Y. Yilmaz, A.S. Yoon, M. Zanetti

University of Minnesota, Minneapolis, USA
S.I. Cooper, P. Cushman, B. Dahmes, A. De Benedetti, G. Franzoni, A. Gude, J. Haupt, S.C. Kao, K. Klapoetke, Y. Kubota, J. Mans, N. Pastika, R. Rusack, M. Sasseville, A. Singovsky, N. Tambe, J. Turkewitz

University of Mississippi, University, USA
L.M. Cremaldi, R. Kroeger, L. Perera, R. Rahmat, D.A. Sanders

University of Nebraska-Lincoln, Lincoln, USA
E. Avdeeva, K. Bloom, S. Bose, J. Butt, D.R. Claes, A. Dominguez, M. Eads, P. Jindal, J. Keller, I. Kravchenko, J. Lazo-Flores, H. Malbouisson, S. Malik, G.R. Snow

State University of New York at Buffalo, Buffalo, USA
U. Baur, A. Godshalk, I. Iashvili, S. Jain, A. Kharchilava, A. Kumar, S.P. Shipkowski, K. Smith

Northeastern University, Boston, USA
G. Alverson, E. Barberis, D. Baumgartel, M. Chasco, J. Haley, D. Trocino, D. Wood, J. Zhang

Northwestern University, Evanston, USA
A. Anastassov, A. Kubik, N. Mucia, N. Odell, R.A. Ofierzynski, B. Pollack, A. Pozdnyakov, M. Schmitt, S. Stoynev, M. Velasco, S. Won

University of Notre Dame, Notre Dame, USA
L. Antonelli, D. Berry, A. Brinkerhoff, M. Hildreth, C. Jessop, D.J. Karmgard, J. Kolb, K. Lannon, W. Luo, S. Lynch, N. Marinelli, D.M. Morse, T. Pearson, R. Ruchti, J. Slaunwhite, N. Valls, J. Warchol, M. Wayne, M. Wolf, J. Ziegler

The Ohio State University, Columbus, USA
B. Bylsma, L.S. Durkin, C. Hill, R. Hughes, P. Killewald, K. Kotov, T.Y. Ling, D. Puigh, M. Rodenburg, C. Vuosalo, G. Williams, B.L. Winer

Princeton University, Princeton, USA
N. Adam, E. Berry, P. Elmer, D. Gerbaudo, V. Halyo, P. Hebda, J. Hegeman, A. Hunt, E. Laird, D. Lopes Pegna, P. Lujan, D. Marlow, T. Medvedeva, M. Mooney, J. Olsen, P. Piroué, X. Quan, A. Raval, H. Saka, D. Stickland, C. Tully, J.S. Werner, A. Zuranski

University of Puerto Rico, Mayaguez, USA
J.G. Acosta, E. Brownson, X.T. Huang, A. Lopez, H. Mendez, S. Oliveros, J.E. Ramirez Vargas, A. Zatserklyaniy

Purdue University, West Lafayette, USA
E. Alagoz, V.E. Barnes, D. Benedetti, G. Bolla, D. Bortoletto, M. De Mattia, A. Everett, Z. Hu, M. Jones, O. Koybasi, M. Kress, A.T. Laasanen, N. Leonardo, V. Maroussov, P. Merkel,

D.H. Miller, N. Neumeister, I. Shipsey, D. Silvers, A. Svyatkovskiy, M. Vidal Marono, H.D. Yoo, J. Zablocki, Y. Zheng

Purdue University Calumet, Hammond, USA
S. Guragain, N. Parashar

Rice University, Houston, USA
A. Adair, C. Boulahouache, V. Cuplov, K.M. Ecklund, F.J.M. Geurts, B.P. Padley, R. Redjimi, J. Roberts, J. Zabel

University of Rochester, Rochester, USA
B. Betchart, A. Bodek, Y.S. Chung, R. Covarelli, P. de Barbaro, R. Demina, Y. Eshaq, A. Garcia-Bellido, P. Goldenzweig, Y. Gotra, J. Han, A. Harel, S. Korjenevski, D.C. Miner, D. Vishnevskiy, M. Zielinski

The Rockefeller University, New York, USA
A. Bhatti, R. Ciesielski, L. Demortier, K. Goulianos, G. Lungu, S. Malik, C. Mesropian

Rutgers, the State University of New Jersey, Piscataway, USA
S. Arora, A. Barker, J.P. Chou, C. Contreras-Campana, E. Contreras-Campana, D. Duggan, D. Ferencek, Y. Gershtein, R. Gray, E. Halkiadakis, D. Hidas, D. Hits, A. Lath, S. Panwalkar, M. Park, R. Patel, V. Rekovic, A. Richards, J. Robles, K. Rose, S. Salur, S. Schnetzer, C. Seitz, S. Somalwar, R. Stone, S. Thomas

University of Tennessee, Knoxville, USA
G. Cerizza, M. Hollingsworth, S. Spanier, Z.C. Yang, A. York

Texas A&M University, College Station, USA
R. Eusebi, W. Flanagan, J. Gilmore, T. Kamon[55], V. Khotilovich, R. Montalvo, I. Osipenkov, Y. Pakhotin, A. Perloff, J. Roe, A. Safonov, T. Sakuma, S. Sengupta, I. Suarez, A. Tatarinov, D. Toback

Texas Tech University, Lubbock, USA
N. Akchurin, J. Damgov, P.R. Dudero, C. Jeong, K. Kovitanggoon, S.W. Lee, T. Libeiro, Y. Roh, I. Volobouev

Vanderbilt University, Nashville, USA
E. Appelt, D. Engh, C. Florez, S. Greene, A. Gurrola, W. Johns, P. Kurt, C. Maguire, A. Melo, P. Sheldon, B. Snook, S. Tuo, J. Velkovska

University of Virginia, Charlottesville, USA
M.W. Arenton, M. Balazs, S. Boutle, B. Cox, B. Francis, J. Goodell, R. Hirosky, A. Ledovskoy, C. Lin, C. Neu, J. Wood, R. Yohay

Wayne State University, Detroit, USA
S. Gollapinni, R. Harr, P.E. Karchin, C. Kottachchi Kankanamge Don, P. Lamichhane, A. Sakharov

University of Wisconsin, Madison, USA
M. Anderson, M. Bachtis, D. Belknap, L. Borrello, D. Carlsmith, M. Cepeda, S. Dasu, L. Gray, K.S. Grogg, M. Grothe, R. Hall-Wilton, M. Herndon, A. Hervé, P. Klabbers, J. Klukas, A. Lanaro, C. Lazaridis, J. Leonard, R. Loveless, A. Mohapatra, I. Ojalvo, G.A. Pierro, I. Ross, A. Savin, W.H. Smith, J. Swanson

†: Deceased
1: Also at CERN, European Organization for Nuclear Research, Geneva, Switzerland

2: Also at National Institute of Chemical Physics and Biophysics, Tallinn, Estonia
3: Also at Universidade Federal do ABC, Santo Andre, Brazil
4: Also at California Institute of Technology, Pasadena, USA
5: Also at Laboratoire Leprince-Ringuet, Ecole Polytechnique, IN2P3-CNRS, Palaiseau, France
6: Also at Suez Canal University, Suez, Egypt
7: Also at Cairo University, Cairo, Egypt
8: Also at British University, Cairo, Egypt
9: Also at Fayoum University, El-Fayoum, Egypt
10: Now at Ain Shams University, Cairo, Egypt
11: Also at Soltan Institute for Nuclear Studies, Warsaw, Poland
12: Also at Université de Haute-Alsace, Mulhouse, France
13: Now at Joint Institute for Nuclear Research, Dubna, Russia
14: Also at Moscow State University, Moscow, Russia
15: Also at Brandenburg University of Technology, Cottbus, Germany
16: Also at Institute of Nuclear Research ATOMKI, Debrecen, Hungary
17: Also at Eötvös Loránd University, Budapest, Hungary
18: Also at Tata Institute of Fundamental Research - HECR, Mumbai, India
19: Now at King Abdulaziz University, Jeddah, Saudi Arabia
20: Also at University of Visva-Bharati, Santiniketan, India
21: Also at Sharif University of Technology, Tehran, Iran
22: Also at Isfahan University of Technology, Isfahan, Iran
23: Also at Shiraz University, Shiraz, Iran
24: Also at Plasma Physics Research Center, Science and Research Branch, Islamic Azad University, Teheran, Iran
25: Also at Facoltà Ingegneria Università di Roma, Roma, Italy
26: Also at Università della Basilicata, Potenza, Italy
27: Also at Università degli Studi Guglielmo Marconi, Roma, Italy
28: Also at Università degli studi di Siena, Siena, Italy
29: Also at University of Bucharest, Faculty of Physics, Bucuresti-Magurele, Romania
30: Also at Faculty of Physics of University of Belgrade, Belgrade, Serbia
31: Also at University of Florida, Gainesville, USA
32: Also at University of California, Los Angeles, Los Angeles, USA
33: Also at Scuola Normale e Sezione dell' INFN, Pisa, Italy
34: Also at INFN Sezione di Roma; Università di Roma "La Sapienza", Roma, Italy
35: Also at University of Athens, Athens, Greece
36: Also at Rutherford Appleton Laboratory, Didcot, United Kingdom
37: Also at The University of Kansas, Lawrence, USA
38: Also at Paul Scherrer Institut, Villigen, Switzerland
39: Also at Institute for Theoretical and Experimental Physics, Moscow, Russia
40: Also at Gaziosmanpasa University, Tokat, Turkey
41: Also at Adiyaman University, Adiyaman, Turkey
42: Also at The University of Iowa, Iowa City, USA
43: Also at Mersin University, Mersin, Turkey
44: Also at Kafkas University, Kars, Turkey
45: Also at Suleyman Demirel University, Isparta, Turkey
46: Also at Ege University, Izmir, Turkey
47: Also at School of Physics and Astronomy, University of Southampton, Southampton, United Kingdom
48: Also at INFN Sezione di Perugia; Università di Perugia, Perugia, Italy

49: Also at University of Sydney, Sydney, Australia
50: Also at Utah Valley University, Orem, USA
51: Also at Institute for Nuclear Research, Moscow, Russia
52: Also at University of Belgrade, Faculty of Physics and Vinca Institute of Nuclear Sciences, Belgrade, Serbia
53: Also at Argonne National Laboratory, Argonne, USA
54: Also at Erzincan University, Erzincan, Turkey
55: Also at Kyungpook National University, Daegu, Korea